UNIVERSIDADE DE LISBOA
FACULDADE DE CIÊNCIAS
DEPARTAMENTO DE FÍSICA

BRINGING PORTAL DOSIMETRY FOR RADIOTHERAPY INTO THE CLINIC

Ana Seabra Gomes Domingos

Mestrado Integrado em Engenharia Biomédica e Biofísica
Perfil em Radiações em Diagnóstico e Terapia

Dissertação orientada por:
Doutor Joep Stroom e Prof. Doutor Luís Peralta

2017

ACKNOWLEDGEMENTS

Firstly, I would like to start by showing my sincere gratitude to my supervisor Joep Stroom from Champalimaud Foundation, who gave me the opportunity to join this project and work in such an amazing environment. I also want to thank him for his encouragement, and for all the support during this internship. Secondly, I would like to give a special thanks to Sandra Vieira, who had opened the doors for me at Champalimaud Foundation, and was a constant present during this journey. I am very grateful for her friendship and advice during the whole process. I am aware that, without Joep's guidance and patient to teach me everything I wanted to know, and without Sandra's constant advice and support, the present thesis wouldn't be possible. Both had taught me a lot and, more than my supervisors, they were real friends to me. I have the most respect for both, and I wish them all the best in this world. I also want to thank Ana Taborda, my postdoc office partner, and a constant support and company during these months. I really appreciate the patient of all the people in the Radiotherapy Department in general but, specially, the guidance and support of Maria João, Milton, Cláudia, and Dalila. It was a pleasure to spend this year at Radiotherapy Department, surrounded by amazing and expert people.

A big thanks to my intern supervisor, Professor Luís Peralta, for all the guidance during this journey. Even though not physically present, he was always present and a constant support. Thank you for all the advices and strength.

Finally, I would like to thank my family, my boyfriend, and my friends. I couldn't ask for a better family and I am really thanked for all the strength during this last year. Thank you for being present and so supportive. To you Guilherme, special thanks for making me believe that was possible and, specially, for not letting me give up. To my friends, thank you for being a distraction and a reason to smile even, and specially, in the most stressful moments of this journey.

RESUMO

Hoje em dia, o cancro é um dos maiores problemas a nível de saúde pública por todo o mundo. A radioterapia tem assumido uma importância cada vez maior, no que concerne a tratamentos do foro oncológico. O objetivo principal da radioterapia prende-se com irradiar o tecido do tumor com uma elevada dose, poupando o tecido normal e saudável circundante o máximo possível, de modo a limitar possíveis complicações durante o tratamento do paciente. De entre os métodos de radioterapia mais utilizados, destacam-se a radioterapia de intensidade modulada (IMRT), e uma nova técnica que constitui uma forma avançada de IMRT, a terapia de arco volumétrico (VMAT). Ao contrário dos tratamentos de IMRT, durante os quais o acelerador (LINAC) roda diversas vezes em torno do paciente, ou faz paragens e recomeços repetidos de forma a irradiar o tumor de diferentes ângulos, nos tratamentos VMAT, a dose é entregue ao tumor por inteiro, durante uma única rotação de 360 ° (tipicamente em menos de dois minutos). Com o crescente uso das técnicas de IMRT e VMAT em ambiente clínico e, consequentemente, com o crescente aumento da complexidade dos planos de tratamento e das doses prescritas (aumento do número de planos hipofracionados e de dose única), a necessidade de procedimentos de controlo de qualidade (QA) tem vindo a aumentar. Por esta razão, os procedimentos de QA rotineiros já não são suficientes e, de modo a detetar possíveis erros, tornou-se necessário desenvolver novos procedimentos de QA.

Os procedimentos de QA incluem a verificação pré-tratamento, onde o procedimento de QA é feito antes do tratamento, aquando a irradiação de um fantoma, e a verificação *in vivo*, onde o procedimento de QA é feito durante o tratamento, aquando a irradiação do paciente. Por questões de segurança, a verificação pré-tratamento é o procedimento de QA mais frequente na maioria das clínicas de radioterapia, permitindo a deteção de erros de forma precoce, dado esta ser feita antes de sujeitar o paciente ao tratamento de radioterapia. No caso da Fundação Champalimaud, a verificação pré-tratamento é feita rotineiramente com recurso a um fantoma constituído por díodos designado ArcCHECK. No entanto, esta solução apresenta grandes desvantagens dado o tempo despendido no procedimento de QA, bem como o peso e a baixa resolução do fantoma em questão. Por essa razão, a possibilidade de introdução e utilização de um dispositivo de imagem portal (EPID) na clínica, que permita otimizar todo o processo de verificação de pré-tratamento, tem vindo a ser estudada.

Os EPIDs foram concebidos e desenvolvidos originalmente com o propósito de verificação da posição do paciente durantes as sessões de radioterapia. No entanto, há mais de uma década, os EPIDs começaram a ser utilizados em contexto clínico, como procedimentos de QA de verificação pré-tratamento no caso de planos de IMRT e VMAT. Atualmente, os EPIDs constituem uma ferramenta avançada de tecnologia digital, que permite melhorias na localização da região alvo, mantendo a eficiência clínica. A dosimetria portal apresenta de facto grandes vantagens, nomeadamente, a aquisição rápida de imagens, a alta resolução, e o potencial para introdução de verificação *in vivo* e verificação de dose a 3D.

Aquando a verificação pré-tratamento de planos IMRT e VMAT, é necessário proceder à verificação de dose, de modo a evitar a subdose do volume alvo, ou a sobredose dos tecidos normais. Assim, diferentes métodos de verificação de dose que permitem a comparação entre as distribuições de dose (a de referência e a medida) têm vindo a ser desenvolvidos e implementados na prática clínica. Um dos métodos de verificação de dose mais utilizado hoje em dia é o método de avaliação gama ou análise gama. Este

método constitui uma ferramenta quantitativa de comparação de distribuições de dose, e permite determinar se os pontos de dose comparados passam ou falham o teste de comparação – é dito que os pontos de dose comparados passam o teste de comparação se o gama for igual ou menor que 1, sendo que, por oposição, os pontos de dose comparados falham o teste de comparação se o gama for maior que 1.

O presente projeto teve como objetivo principal, a implementação clínica e rotineira do EPID para verificação pré-tratamento, com vista à substituição dos procedimentos de QA realizados com recurso ao ArcCHECK. Para tal, diferentes estudos foram conduzidos em diferentes LINAC (TrueBeam™ e Edge™). Inicialmente, compararam-se os resultados obtidos aquando a utilização da solução de dosimetria portal desenvolvida pela Varian para verificação pré-tratamento, com os resultados obtidos aquando da utilização do ArcCHECK, para ambos os LINAC. No sentido de testar e comparar a sensibilidade de ambos os sistemas (EPID e ArcCHECK) durante a verificação pré-tratamento, foram também levados a cabo estudos com vista à introdução de erros nos planos dos pacientes. Finalmente, de forma análoga, introduziram-se diferentes tipos de erro no plano de um paciente, de forma a avaliar os efeitos destes ao nível dos órgãos de risco (OARs).

No que respeita aos primeiros testes, estabelecendo um critério de análise gama com uma diferença de dose de 3%, e uma distância de concordância (DTA) de 3mm, concluiu-se, para o LINAC TrueBeam™, que os resultados obtidos aquando da verificação pré-tratamento eram melhores quando se usava o ArcCHECK, e piores quando se usava o EPID. Já para o LINAC Edge™, o contrário foi verificado no sentido em que os resultados obtidos aquando da verificação pré-tratamento se revelaram melhores para o EPID, e piores para o ArcCHECK. Esta discrepância pode ser explicada tendo em conta os diferentes EPID incorporados em cada um dos diferentes LINAC, sendo que o LINAC Edge™ tem provavelmente um melhor EPID (mais recente) que o LINAC TrueBeam™. Aquando os testes de introdução de diferentes tipos de erros (MUs, posição do MLC – aleaórios e sistemáticos-, e ângulo do colimador) nos ficheiros XML contendo os planos dos pacientes, para uma análise gama 3 %/3 mm, concluiu-se que o EPID era sensível aos diferentes tipos de erros dado que, quanto maior a magnitude do erro introduzido, pior a irradiação, e, consequentemente, piores os resultados obtidos. Em comparação com o ArcCHECK, o EPID demonstrou-se igualmente sensível, permitindo, no entanto, resultados mais coerentes. Finalmente, a influência dos diferentes tipos de erros introduzidos nos órgãos em risco foi de encontro ao esperado na medida em que, quanto maior a magnitude do erro introduzido, maiores os valores de diferença obtidos a nível de volumes e, consequentemente, menores os valores de gama, e maiores os efeitos nos órgãos em questão.

No final, a análise de resultados demonstrou e veio confirmar as claras vantagens do EPID face ao ArcCHECK, dado que este permitiu melhores resultados, demonstrando-se, ao mesmo tempo, mais sensível a erros introduzidos nos planos dos pacientes. No entanto, mais estudos devem ser conduzidos no sentido de testar mais casos clínicos com tumores presentes em diferentes localizações e diferentes fracionamentos. Em todo o caso, devido aos resultados promissores obtidos durante este projeto, pela primeira vez na Fundação Champalimaud, o EPID começou a ser usado de forma rotineira para verificação pré-tratamento num dos LINAC disponíveis (LINAC Edge™), substituindo os antigos e pouco vantajosos procedimentos de QA feitos com recurso ao ArcCHECK. Esta nova prática clínica e, ao fim ao cabo, mudança de paradigma, apenas vem encorajar a continuação dos estudos para implementação de procedimentos de QA com o EPID para verificação pré-tratamento nos restantes LINAC disponíveis na Fundação Champalimaud,

bem como estimular a implementação de procedimentos de QA, também com recurso ao EPID, mas para verificação *in vivo*.

Palavras-Chave: Tumor; Controlo de Qualidade; Dosimetria Pré-tratamento; Dosimetria EPID; Análise Gama.

ABSTRACT

Nowadays, cancer is one of the major public health problems around the world. Radiotherapy is one of the most widely used cancer treatment method, and, among the most commonly used radiotherapy methods, are intensity modulated radiotherapy (IMRT), and a novel radiation technique called volumetric modulated arc therapy (VMAT), which is an advanced form of IMRT. With the increased use of IMRT and VMAT, and, consequently, increasing in treatment plans complexity, as well as higher dose prescriptions, the demand for patient-specific quality assurance (QA) procedures has increased, in order to avoid major errors. Thus, recommended QA procedures might no longer be sufficient and new procedures are necessary to detect possible errors.

Patient-specific quality assurance includes both pre-treatment verification, where the QA procedure is done before the treatment, with a phantom, and *in vivo* verification, where the QA procedure is done during the treatment, with the patient. For a question of safety, in clinical practice, pre-treatment patient-specific QA procedures are more common, once they allow the early detection of errors, prior to the radiotherapy treatment. At Champalimaud Foundation, the pre-treatment patient-specific QA is performed routinely using a cylindrical detector array called ArcCHECK. However, due the cumbersome and low-resolution of ArcCHECK, Electronic Portal Image Device (EPID) has been studied. EPIDs provide an advanced tool with digital technology to improve target localization and maintain clinical efficiency. EPID dosimetry has a lot of advantages such as fast image acquisition, high resolution, digital format, and potential for *in vivo* measurements and 3D dose verification, which make it a very promising tool.

The main goal of this project was to examine the clinical introduction of EPID for pre-treatment dosimetry, in order to replace ArcCHECK QA measurements and bring into the clinic the routinely use of EPID to perform QA measurements. For that, different studies were conducted on both TrueBeam™ and Edge™ LINAC, where the performance of the portal dosimetry solution (Portal Dosimetry software developed by Varian) for pre-treatment patient-specific QA of IMRT and VMAT plans was compared with ArcCHECK. Moreover, errors were introduced in the patient plans in order to study and compare the sensitivity of both EPID ArcCHECK during pre-treatment patient-specific QA, and evaluate the effects of the different types of error in the organs at risk.

Regarding the first tests, for a gamma analysis with a dose-difference criterion of 3 % and distance-to-agreement (DTA) of 3 mm, on the TrueBeam™ LINAC, we have obtained better results with ArcCHECK, while, on the Edge™ LINAC, we have obtained better results with EPID. This discrepancy can be explained by the different a-Si EPIDs incorporated on the two LINACs – the Edge™ LINAC has probably a better EPID than the TrueBeam™ LINAC. Regarding the introduction of errors (MUs, MLC position - random and systematic -, and collimator angle) in the XML files with the patient plans, for a 3 %/3 mm gamma analysis, we have concluded that EPID is sensitive to the different types of error introduced. When comparing EPID sensitivity with ArcCHECK sensitivity, the results obtained suggested that EPID is

as sensitive as ArcCHECK and, on top of that, shows more coherent results. Finally, when verifying the influence of the introduced errors in the organs at risk (OARs), we have obtained, as expected, that, higher the magnitude error introduced, higher the volume difference values, consequently, lower the gamma passing rate values, and higher effects in the organs at risk.

In the end, the analysis of the results showed that EPID, at the same time, allows better results, and is more sensitivity, than ArcCHECK. However, more clinical cases, considering several treatment sites and with different fractionation schemes, should be studied with both portal dosimetry and ArcCHECK to verify the obtained results. Due to the very promising results obtained, for the first time at Champalimaud Foundation, EPID had started to be routinely used in pre-treatment patient-specific QA on Edge™ LINAC. Therefore, this only encourages the continuation of the study for implementation of pre-treatment patient-specific QA with EPID on the Varian TrueBeam™ LINAC, as well as the implementation of *in vivo* patient-specific QA.

Key- words: Tumor; Quality Assurance; Pre-Treatment Dosimetry; EPID Dosimetry; Gamma Analysis.

TABLE OF CONTENTS

LIST OF TABLES

LIST OF FIGURES

LIST OF ABBREVIATIONS

2D Two-Dimensional

3D Three-Dimensional

a-Si EPID amorphous-Silicon EPID

BP Beam Profile

BEV Beams Eye View

CCD-based EPID Camera-based EPID

CCW Counterclockwise

CRT Conformal Radiation Therapy

CT Computed Tomography

CTV Clinical Target Volume

CU Computer Units

CW Clockwise

DD Dose Difference

DF Dark-Field

DICOM Digital Imaging and Communication in Medicine

DMLC Dynamic MLC

DTA Distance-to-Agreement

DVH Dose-Volume Histogram

EPD Electronic Portal Dose

EPID Electronic Portal Imaging Device

FF Flood-Field

FFF Flattening Filter Free

GTV Gross Tumor Volume

IGRT Image-Guided Radiation Therapy

IMAT Intensity Modulated Arc Therapy

IMRT Intensity Modulated Radiotherapy

ITV Internal Target Volume

LINAC Linear Accelerator

LQ Linear-Quadratic

MeV Mega Electron Volt

MLC Multi-Leaf Collimator

MRI Magnetic Resonance imaging

MU Monitor Units

MV Megavoltage

OAR Organ at Risk

PDD Percentage Depth Dose

PDI Portal Dose Image

PDIP Portal Image Dose Prediction

PRV Planning Organ at Risk Volume

PTV Planning Target Volume

QA Quality Assurance

RF Radiofrequency

SAD Source-axis distance

SMLC Segmented MLC

SRS Stereotactic Radiosurgery

SSD Source-Surface Distance

TLD Thermoluminescent Dosimeter

TPS Treatment Planning System

VMAT Volumetric Modulated Arc Therapy

XML Extensible Markup Language

CHAPTER 1. INTRODUCTION

1.1 Motivation

At the Radiotherapy Department of Champalimaud Foundation, we currently have two different treatment systems (Elekta and Varian), each one of them with their own portal dosimetry software (PDAPP and Portal Dosimetry, respectively). Besides these two software, a software called PreDose, that does pre-treatment and *in vivo* dosimetry at the EPID level for the Elekta machines, has been developed, and a new *in vivo* dosimetry software from MAASTRO (Netherlands), for the Varian machines, has just arrived to be tested.

Despite the existence of these four software, none of them is being routinely used in the clinic due to the absence of their full implementation. At the moment, individual patient plan QA is performed pre-treatment by the more cumbersome and low-resolution ArcCHECK (SunNuclear®), which uses diode arrays for performing measurements.

In the case of this project, I will focus my attention on the Varian system, leaving the Elekta system aside. The main goals of the present project are to finalize measurements and comparisons and test new software versions, compare EPID dosimetry data with ArcCHECK data for many patients, and determine the sensitivity of one of the Varian systems by purposely introducing errors in a set of test plans. When satisfactory results are obtained, clinical procedures and criteria for Varian systems will be developed, and pre-treatment dosimetry with EPID (Portal Dosimetry) is going to replace ArcCHECK measurements, in order to improve the accuracy of QA measurements and the efficiency at the Radiotherapy Department of Champalimaud Foundation.

Thus, this project which aims to replace ArcCHECK QA measurements and bring into the clinic the routine use of EPID to perform QA measurements, is of utmost importance once it will greatly facilitate and improve the operation of the clinic.

1.2 Contextualization

Cancer is one of the major public health problems in Europe, in the United States, and other countries in the western world [1].

Radiotherapy is one of the main treatment methods for cancer along with surgery, chemotherapy, and hormone therapy, once it (alone or in combination with other treatments) is a curative treatment for 40

% of the cancer patients receiving it. Among the most commonly used radiotherapy methods are 3D conformal radiation therapy (3D CRT), intensity modulated radiotherapy (IMRT), and particle beam therapy [1].

Intensity modulated radiotherapy (IMRT) is an advanced mode of high-precision radiotherapy which offers a dose distribution improvement by modulating the two-dimensional X-ray fluence. It uses computer-controlled linear accelerators to deliver precise radiation doses to a malignant tumor or specific areas within the tumor [2][3].

With the increased use of intensity modulated radiotherapy and, consequently, increasing in treatment plans complexity, and higher dose prescriptions, the demand for patient specific verification has increased. Besides that, the possibility of deviations from the plan dose during the treatment planning process and data transfer problems, make it more difficult to discover possible errors. Due to this increasing need for patient specific verification, recommended QA procedures might no longer be sufficient and, therefore, new procedures are necessary to detect possible errors. Films and EPIDs are generally used for this purpose [3].

Electronic portal imaging devices (EPIDs) provide an advanced tool with digital technology to improve target localization and maintain clinical efficiency. Therefore, they can eventually be used for intensity modulated radiation therapy (IMRT) QA. In fact, not long after their clinical introduction for set-up verification, it was realised that EPID images contain dose information. Consequently, several groups started to investigate the dosimetric characteristics of various types of EPID. Nowadays, in some places, EPIDs have gone on to replace traditional dosimetry devices in the clinic for plan verification. EPID dosimetry has a lot of advantages such as fast image acquisition, high resolution, digital format, and potential for *in vivo* measurements and 3D dose verification, which make it a very promising tool [2][4][5].

CHAPTER 2. BACKGROUND

2.1 External Beam Radiotherapy

Radiotherapy is one of the most widely used cancer treatment method. The goal of radiotherapy is to irradiate tumor tissue with a high dose while sparing the surrounding normal healthy tissue as much as possible to limit the complications of a patient treatment.

Depending on the location of the radiation source, internal and external beam radiotherapy can be distinguished. Once internal beam radiotherapy uses radioactive sources placed on the surface or inside of the patient in a very close location of the tumor, external beam radiotherapy uses ionising radiation sources placed at a distance from the patient. In general, nowadays, irradiation is done by using external beam radiotherapy or brachytherapy [1].

Brachytherapy is an advanced cancer treatment where radioactive seeds or sources are placed in or near the tumor itself, giving a high radiation dose to the tumor while reducing the radiation exposure in the surrounding healthy tissues. The term "brachy" is Greek and means “short distance” [6].

In case of external beam radiotherapy, a radiation beam is pointed at a particular part of the body. By using multiple beams in an optimum beam angle configuration, the dose in healthy tissue can be diminished. Different types of radiation have different interactions with tissue, and will cause more or less biological damage. The most commonly ionising radiation types used in external beam radiotherapy are megavoltage X-rays (megavolt or MV photon beams), electrons and protons, produced by a LINAC (linear accelerator).

At the Radiotherapy Department of Champalimaud Foundation, the external beam radiotherapy is accomplished by using megavoltage X-rays, MV photon beams in particular. Clinical megavoltage X-rays beams typically have an energy range between 10 kVp and 50 MV, and are the result of the deceleration of electrons with kinetic energies between 10 keV and 50 MeV in special metallic targets. A major part of electron’s kinetic energy is converted in the target into heat, while a small fraction of the energy is emitted in the form of X-ray photons [7].

External beam radiotherapy is based on interactions of ionizing radiation with matter, and its goal is to eliminate the reproductive capacity of the cells. Thus, to fully understand the effectiveness of external beam radiotherapy in cancer treatment, it is essential to understand the inherent radiobiological principles.

2.1.1 Radiobiological Principles

In order to control tumor volume while preserving the integrity of the healthy tissues, fractionated radiotherapy schemes have been widely prescribed. Conventional fractionation schemes comprise administering 1.2 to 2.0 Gray (Gy) per fraction, 5 days per week, giving a total dose between 60 and 70 Gy which varies according to the tumor volume and the maximum dose that the adjacent healthy tissues tolerate.

The effect of radiation administrated in fractionated schemes is governed by five radiobiological principles, known as the 5R's: (1) Repair of sublethal damage, (2) Repopulation of cells after radiation, (3) Redistribution of cells in the cell cycle, (4) Reoxygenation of the surviving cells and (5) Radiosensitivity of tumor cells [8][10][11].

The first radiobiological effect (repair of sublethal damage), describes the capacity of the cells in repairing sublethal damage induced by radiation, returning to the initial sensitivity values. While health cells exhibit a high capacity to repair sublethal damage, tumor cells exhibit a low capacity to repair sublethal damage, leading to the accumulation of irreversible damage, and causing cell death. It is important to note that the rate of the repair damage induced by radiation is directly related to several factors including the dose per fraction, and the nature of the tissues and cells [8][10].

The second radiobiological effect (repopulation of cells after radiation) is the process by which healthy cells irreversibly damaged or killed are replaced by cell proliferation after a fraction [8].

The third radiobiological effect (redistribution of cells in the cell cycle), refers to the process in which cells progress through the cell cycle reaching the most sensitive stage of radiation. As known, the sensitivity of the cells varies according to the stage of the cell cycle. For example, in mitosis, cells are more sensitive to radiation since the DNA compaction makes it more susceptible to the damaging effects of radiation as well as less accessible to the repair enzymes. Tumor cells have a high mitotic rate (greater proliferative capacity) and, therefore, are considered more radiosensitive than healthy tissues. As a result, fraction to fraction, there is a higher proportion of the surviving tumor cells in the mitosis stage [8].

The fourth radiobiological effect (reoxygenation of the surviving cells) corresponds to the process by which the hypoxic cells become oxygenated after irradiation. The more oxygenated areas of the tumors are located at the periphery, while the less oxygenated areas are in central regions. Therefore, once as more oxygenated tumors, more radiosensitive they are considered, after a fraction, cells at the periphery will die more quickly, being the oxygen redirected to neighboring cells with low oxygen content. This results in an increase of oxygenated tumor cells in the next fraction - reoxygenation of the surviving cells [8].

Finally, the last radiobiological effect (radiosensitivity of tumor cells) is considered an intrinsic factor and it is modelled by the linear-quadratic (LQ) equation. The LQ is used to calculate the effects for different fractionated irradiation schemes comprising dose and fraction number [9][10].

In recent years, a significant interest in hypofractionated schemes, higher than 2.5 Gy per fraction, has been observed mainly influenced by the clinical results obtained by stereotactic radiosurgery (SRS). Some studies conducted with high-dose fractionated schemes concluded that the capacity of healthy cells to repair sublethal damage is significant during the treatment session, which is more prolonged in hypofractionated or single shot schemes than in conventional schemes, enabling to healthy cells to return to the initial sensitivity values. Tumor irradiation in a single fraction prevents cell cycle redistribution and tumor cells death in the cell cycle phases where they are irradiated. The repopulation of tumor cells during treatment is also negligible since the treatment is completed within 1 or 2 weeks. For tumors treated with a

single fraction or extremely high-dose fraction, vascular damage is so extensive that the intra-tumor environment is drastically changed leading to indirect cell death. Consequently, the LQ model is inapplicable when tumors are treated with doses higher than 10 Gy in a single fraction, being only considered when tumors are treated with hypofractionated schemes with doses smaller than 10 Gy per fraction [9][10][11].

2.1.2 LINAC (Linear Accelerator)

A linear accelerator (LINAC) customizes the radiation field (high energy X-rays) according to the tumor's shape, and destroys cancer cells, while sparing surrounding normal tissue. It is the most common device used to treat cancer with external beam radiation. Despite its own several built-in safety measures that ensure that a higher dose than the prescribed one will not be delivered, it must be routinely checked to ensure that it is working properly [12][13].

Medical LINACs are cyclic accelerators that use radiofrequency (RF) waves to accelerate charged particles (electrons) to high energies. In this, the electrons collide with a heavy metal target to produce energy X-rays [14].

In the case of the LINACs at the Radiotherapy Department of Champalimaud Foundation, the charged particles used are electrons. The electrons are accelerated in a linear path inside special evacuated structures called accelerating waveguides and, to produce the high-power RF fields needed for electron acceleration, special evacuated devices called magnetrons and klystrons are used. Basically, the accelerated electrons collide with a primary target, being decelerated, and emitting braking radiation (bremsstrahlung), which will result in the production of X-rays. The X-rays produced are then customized either by blocks positioned in the head of the LINAC or by a multi-leaf collimator incorporated in the head of the LINAC [7][13]. A scheme of this process is shown in the figure below, **Figure 2.1**.

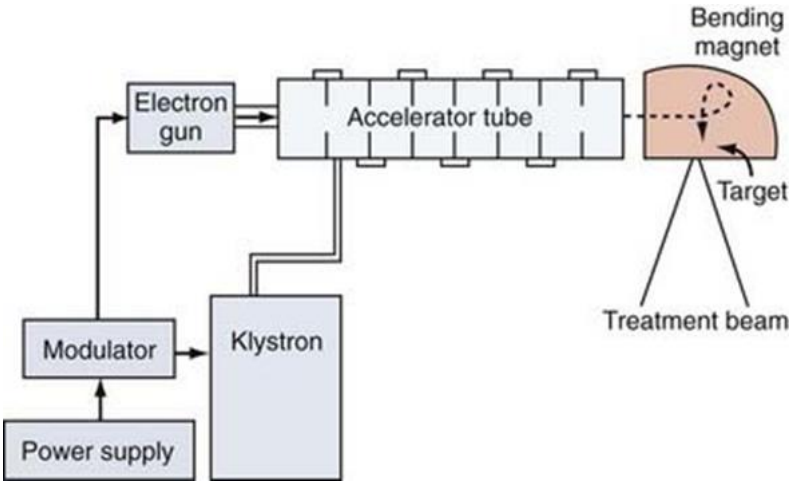

Figure 2.1. Production of high energy X-rays by the LINAC. Retrieved from [15].

As said before, the LINACs available at the Radiotherapy Department are three - Edge™ and TrueBeam™ LINAC, from Varian, and Synergy™ LINAC, from Elekta. The TrueBeam™ LINAC is an advanced image-guided radiation therapy (IGRT) system used to treat cancer with speed and accuracy while avoiding healthy tissues and organs. TrueBeam™ was designed for complex cases of cancer of the lung, breast, stomach, and brain. It can also be used for cases of cancers of the liver and prostate, along with other cancers treated with radiation therapy. The Edge™ LINAC was the latest addition and it is a state-of-the-art linear accelerator coupled with real-time motion management to ensure fast and precise delivery of treatment. It has the highest dose rate in the industry allowing for faster treatments. The quality and safety system of the Edge™ performs accuracy checks every 10 milliseconds to ensure quality of care. Finally, the Synergy™ LINAC was the first linear accelerator to bring 3D image guidance into the treatment set up process and was the first being acquired at the Radiotherapy Department of Champalimaud Foundation. The main difference between these three LINAC is the characteristics of the multi-leaf collimator (MLC) incorporated in the LINAC that make them more appropriate for some cases than for the others.

One important aspect to be referred is that the LINAC output is measured in terms of some special units called monitor unit (MU), using two ionisation chambers. Thus, the first ionisation chamber measures the MU and stops the beam when the pretended radiation it is completely delivered, while the second ionisation chamber provides a backup in case of failure of the first chamber.

MU (Monitor Unit)

As mentioned before, monitor unit (MU) is a measure of a machine output such as a LINAC. The most common definition, and the one used in this thesis, is that the ionisation chamber reads 1 MU when an absorbed dose of 1 cGy is delivered to a point at a given depth in the phantom, with the surface of the phantom positioned so that the specified point is at the isocentre of the machine and the field size is 10 cm × 10 cm at the isocentre. This is an important measurement, as the output of the linear accelerator can only be read in charge passing through the ionisation chamber.

2.1.3 MLC (Multi-Leaf Collimator)

Multi-leaf collimators (MLCs) are an addition to LINAC dose delivery technology. They are beam shaping devices used as a replacement for collimator blocks and, without them, the LINAC would only be capable of treating quadrangular or rectangular treatment fields. Each leaf in the MLC has, typically, a width at the isocenter ranging from 0.5 cm to 1 cm, and can be individually moved to match each treatment plan and enhance dose delivery. A MLC incorporate from 20 to 60 pairs of narrow closely abutting tungsten leaves. [7]

The MLCs may be an integral part of the LINAC head, replacing upper or lower secondary collimator jaws, or may be attached to the LINAC's head and used in conjunction with both the upper and

lower collimator jaws. In the figure below, **Figure 2.2**, there is a typical MLC attached to a LINAC head and used in conjunction with the upper and lower collimator jaws.

Figure 2.2. MLC with 60 pairs of abutting tungsten leaves (TrueBeam™ MLC, Varian). Adapted from [16].

On the one hand, the advantages of an MLC include simple and less time-consuming preparation, ability to treat multiple fields without re-entering the treatment room, simple change or correction of field shape, lower therapy expenses once individual shielding block are not need and, therefore, there is no need to handle the toxic wood's alloy, shorter therapy time, and continuous adjusting of field shape during irradiation in advanced conformal radiotherapy. On the other hand, the disadvantages of an MLC include the discrete step size of the leaves resulting in stepping edge effect, additional quality assurance requirements, additional data to characterize the output factors, wider penumbra (the penumbra is the region at the edges of the radiation beam where the dose rapidly decreases), radiation leakage through and between leaves, and, eventually, problems with generating some complex field shapes [7].

2.1.4 IMRT (Intensity Modulated Radiotherapy)

IMRT is currently one of the most advanced form of conformal radiotherapy, and is being used most extensively to treat cancers of the prostate, head and neck, and central nervous system. It is also being used to treat cancers of the breast, thyroid, and lung, as well as gastrointestinal and gynecologic malignancies, and certain types of sarcoma [7][17].

This technique uses computer-controlled linear accelerators to deliver precise radiation doses to a malignant tumor or specific areas within the tumor, and allows for the radiation dose to conform more precisely to the three-dimensional shape of the tumor. Thus, beams of radiation are guided to the tumor from many different angles and, at each of these angles, the intensity of the radiation is modulated, and the shape of the beam is changed to match the shape of the tumor [7][18].

In comparison with conventional techniques, IMRT allows higher and more effective radiation doses to be safely delivered to tumors, with fewer side effects. Besides that, IMRT has the potential to

reduce treatment toxicity, even when doses are not increased. However, due to its complexity, IMRT does require slightly longer daily treatment times, additional planning, and safety checks before the patient can start the treatment [7][17][18].

Various approaches to IMRT have been developed. MLC based IMRT techniques are the most currently used and can be divided in two categories: one uses multiple static MLC shaped fields, and the other uses dynamic MLC dose delivery approaches. In IMRT treatments, the MLC can be operating in one of three basic modes: the segmented MLC (SMLC) mode (static IMRT), often referred to as step and shoot mode, where there is no MLC motion while the beam is on; the dynamic MLC (DMLC) mode (dynamic IMRT), sometimes referred to as the sliding window mode, where the intensity modulated fields are delivered in a dynamic mode with the leaves of the MLC moving during the irradiation of the patient; and the intensity modulated arc therapy (IMAT), where the sliding window approach is used as the gantry rotates around a patient [7].

Nowadays, a novel radiation technique called volumetric modulated arc therapy (VMAT) is being increasingly used by the clinical worldwide. VMAT is an advanced form of IMRT that delivers a precisely-sculpted 3D dose distribution with a 360-degree rotation of the gantry in a single or multi-arc treatment. Thus, this technique differs from existing techniques, such as IMAT, once it delivers to the whole volume, rather than slice by slice [19].

Unlike conventional IMRT treatments, during which the machine must rotate several times around the patient, or make repeated stops and starts to treat the tumor from many different angles, VMAT can deliver the dose to the entire tumor in a 360-degree rotation, typically in less than two minutes. Thus, the advantages of VMAT include highly conformal dose distributions with improved target volume coverage, while sparing normal tissues, as well as reduced treatment delivery time [19][20].

2.1.5 FFF Beams

The improvement of IMRT and VMAT, as well as the development of new radiotherapy schemes where large MUs are often required, have increased the interest in operating the LINAC in a flattening filter free (FFF) mode.

The main benefit of FFF beams relies on the possibility of deliver higher dose rates, requiring a shorter delivery time. Less delivery time means that the patient is on the treatment couch for a shorter period, which will improve patient comfort and decrease the possibility of inaccuracies due patient movement.

2.2 Clinical Procedure in Radiotherapy

2.2.1 Radiotherapy Chain

In radiotherapy, each clinical process is complex and involves several steps as illustrated in **Figure 2.3.**

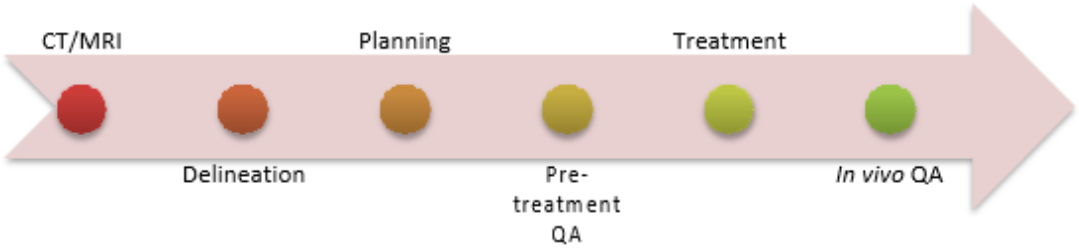

Figure 2.3. Radiotherapy chain for each clinical process.

First, the radiation oncologist evaluates the disease stage, and decides between a curative and a palliative treatment. Depending on the characteristics of the tumor, the treatment, or combination of treatments, is decided (radiotherapy, chemotherapy, etc.). If the treatment chosen is radiotherapy, the process starts with imaging the patient's anatomy at the tumor site using computed tomography (CT), and sometimes magnetic resonance imaging (MRI), to enhance the soft tissue contrast. Then, the radiation oncologist delineates the target volume as organs at risk (OARs) from the acquired CT, and defines the dose to be prescribed with the support of a treatment planning system (TPS). After the delineation, the next step is to calculate the dose and optimize the dose distribution obtained. This is done by dosimetrists using a TPS. The dose distribution is then evaluated by a physicist that verifies the dose restrictions to the healthy tissue and to the target volume. One way of doing this is to use dose-volume histograms (DVHs) which are a valuable tool that summarize the information contained in the 3D dose distributions and, consequently, can be used to verify if the prescribed dose correctly covers the target volume, and if the irradiation of the OARs doesn't exceed the international recommendations. Finally, the radiation oncologist decides if the plan meets all the aims and restrictions defined, or if a new plan is needed. If the plan is approved, the treatment can start. Before the treatment, a pre- treatment QA is done with the support of a phantom or EPID and, only if the QA gamma passing rate obtained is high enough (higher than a certain established limit value, usually 90 %), the patient is treated. Note that in cases that the QA gamma passing rate is under the established limit value, a new plan has to be done, and the patient is said to be replanned. Preferably, during the treatment, *in vivo* QA is performed using EPID to check the dose actually received by the patient.

Delineation

In the delineation step, the radiation oncologist contours, generally manually and slice-by-slice, the organs at risk (OARs), and the target volumes. OARs are critical normal tissue structures which might be significantly damaged by the radiation depending on the tumor site (for example, for prostate patients, the OARs would be the bladder, the rectum, and the right and left femur head). The target volumes include: the gross tumor volume (GTV), the clinical target volume (CTV), the internal target volume (ITV), and the planning target volume (PTV) (see **Figure 2.4**). The GTV is based on the information obtained from the combination of image, diagnose, and clinic examination modalities. The CTV often includes the area that surrounds directly the GTV, and can contain microscopic diseases and other areas considered to be at risk and needing treatment. The ITV consists in the CTV plus an internal margin drawn to take in account variations in the size and position of the CTV regarding the patient's referential, as well as the internal

movements. Finally, the PTV includes the internal target margin and an additional margin to uncertainties in the configuration, machine tolerations, and intra-treatment variations.

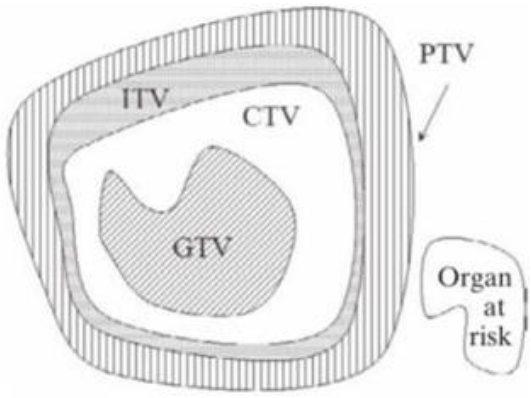

Figure 2.4. Graphical representation of the volumes of interest: the gross tumor volume (GTV), the clinical target volume (CTV), the internal target volume (ITV), and the planning target volume (PTV). Retrieved from [7].

In the figure below, **Figure 2.5**, we can see an example of a CT of a patient with a tumor in the right breast, and the contouring of the target volumes and OARs.

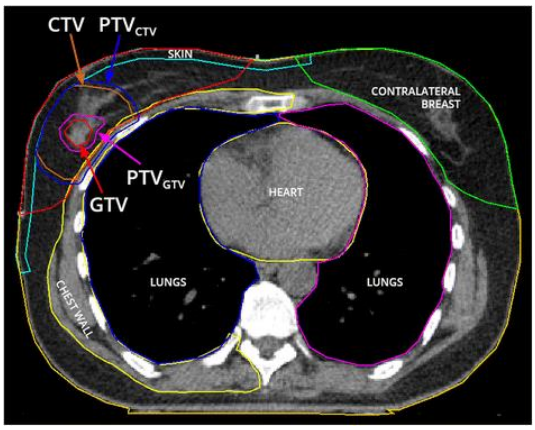

Figure 2.5. CT of a left breast cancer patient with the OAR (heart), the PTV, and the CTV contoured. Retrieved from [26].

Planning

After the delineation, the dosimetrist has to calculate the dose and optimize the dose distribution obtained. For that, it uses a treatment planning system (TPS) that determines the beam geometry to obtain the desired dose to the target volumes, while sparing the organs at risk. An example of this procedure is shown in **Figure 2.6** where the two fields irradiating the PTV and the dose distribution are calculated by the TPS.

Figure 2.6. Determination of the beam geometry by the TPS. Retrieved from [27].

The dose distribution is then evaluated by a physicist that verifies the dose restrictions to the healthy tissue and to the target volume using a TPS.

Treatment Planning System

At the Radiotherapy Department of Champalimaud Foundation, Eclipse™ is the TPS used for the Varian machines, while Monaco™ is the TPS used for the Elekta machine.

Eclipse™ is a software from Varian that provides an interface for treatment planning including contouring of the structures, beam planning, dose calculation, and plan evaluation. Its calculations rely on the beam data describing the output of the machine and several algorithms can be used to calculate the dose [25].

Monaco™ is a software from Elekta that delivers high performance and high precision radiotherapy treatment planning for photon and electron based plans. It combines Monte Carlo and collapsed cone algorithms, handling very complex plans with high accuracy [30].

Pre-Treatment vs In Vivo Patient-Specific QA

In the case of the Radiotherapy Department of Champalimaud Foundation, the pre-treatment patient-specific QA is still performed routinely with the support of ArcCHECK in the three LINAC available (TrueBeam™ and Edge™, Varian, and Synergy™, Elekta), and the *in vivo* QA is only performed sporadically in one of the LINAC available (Synergy™, Elekta). That is the reason why this project is so important, and the implementation of portal dosimetry in all the available LINAC is so needed.

2.2.2 Quality Assurance

The use of IMRT and VMAT in clinical routine is spreading rapidly, and the possibility of treating, simultaneously, different target volumes, with different fractionations, is opening new possibilities.

However, a practical drawback on the implementation of IMRT into the clinical routine remains the time-consuming patient specific quality assurance (QA) that precedes the actual treatment [21][22].

Patient specific quality assurance (QA) is an essential step to guarantee accurate patient treatment in radiotherapy, and is performed at various levels starting with the QA of machine- related parameters such as beam flatness and stability, accuracy of the leaf positions of a multi- leaf collimator (MLC), and accurate modelling of the LINAC at the commissioning stage of the treatment planning system (TPS).

When administering radiotherapy in a fractionated manner (i.e., giving every day a small dose of radiation), a small difference in biological radiation sensitivity between tumor and healthy tissue can be exploited to increase the overall tumor dose, increasing tumor control probability with acceptable normal tissue complication probability. Consequently, every fraction must be given in a reproducible way, and the dose delivery in a patient should be as close as possible to the prescribed dose calculated with the TPS. To achieve a high accuracy in absorbed dose delivery, it is of utmost importance that the dose delivery is verified during external MV photon beam treatment [23].

Dose verification can be accomplished in many ways. The most widely used form of pre- treatment QA for IMRT generally consists of dose measurements (with film, ionization chamber, diode, TLD, etc.) combined with isodose measurements in a phantom, or even by means of gel dosimetry. Radiographic and radiochromic films can be used to verify dose distributions in two dimensions and have a high spatial resolution (i.e., higher ability to differentiate two objects). Once in IMRT treatments we have the presence of high dose gradients in the plane of the beam, films have been especially used for the verification of these types of treatments. However, films have some disadvantages that include the time-consuming dose evaluation and the possibility of errors during processing, digitizing and analysing. Other dosimetry system currently available to perform dose verification is gel dosimetry. Gel dosimetry allows a measurement of the 3D dose distribution but is limited by the complex preparation process and the expensive analysis using a magnetic resonance (MRI) scanner. Finally, a more efficient tool for pre-treatment patient-specific QA is the electronic portal imaging device (EPID). These types of dosimetry device are already attached to the LINAC, providing real-time digital feedback to the user, with no need of additional hardware to perform portal dosimetry. EPID measurements can be performed with minimum set-up requirements, and a 2D dose conversion can be done immediately using the digital images. Although an EPID image contains 2D and not 3D information, it is still possible to reconstruct the 3D dose distribution inside a patient by using a back-projection procedure of the measured portal dose image (PDI) into three dimensions. For a typical pre-treatment patient-specific QA scenario by means of a portal imager, two requirements must be met: firstly, a proper acquisition mode must be available to detect all dose deposited in the imager during irradiation of the treatment field; secondly, one needs to be able to predict what the integrated portal dose image should look like for correct delivery of the fluence distribution [23][24].

ArcCHECK

At Champalimaud Foundation the pre-treatment patient-specific QA is performed using a cylindrical detector array called ArcCHECK (©SunNuclear), which uses 2D matrix of diodes arrays for performing measurements. ArcCHECK displays beams eye view (BEV) dose distribution throughout the entire arc delivery, and the diode arrays are always facing the delivery beam regardless of gantry angle, i.e., the detector geometry relative to the BEV remains constant.

Besides its recurrent use, ArcCHECK it is not the best option once it has a low resolution, and makes the pre-treatment patient specific QA a time-consuming and cumbersome procedure. In this line of thought, it becomes essential to optimize the pre-treatment patient-specific QA procedure currently performed at Champalimaud Foundation to detect more accurately possible errors and to decrease the time dispensed by the physics. This assumes even more importance if we take in consideration that 24 % and 35 % of total treatments conducted in both Varian LINAC have hypofractionated and single shot schemes, respectively.

2.3 EPD (Electronic Portal Dosimetry)

Electronic portal image devices (EPIDs) were originally designed and developed for visual inspection of patient set-up during radiotherapy sessions. However, for over a decade, the electronic portal imaging device (EPID) has undergone extensive development and use as a dosimeter for intensity modulated radiotherapy (IMRT) patient specific quality assurance (QA). Patient specific quality assurance includes both pre-treatment verification and *in vivo* dosimetry [24][31].

2.3.1 EPID (Electronic Portal Imaging Device)

The published literature suggests that the development and use of electronic portal image devices (EPIDs) began in the 1950s. EPIDs can be distinguished mainly according with two categories: optical systems and non-optical systems.

Regarding the optical systems, one pioneering system developed was a camera based EPID that comprised an X-ray image intensifier tube whose light output was optically coupled via a mirror-lens arrangement to a Vidicon TV camera (Strandqvist et al 1958, Wallman et al 1958). A similar system developed consisted of a fluorescent screen coupled to an Orthicon camera via a mirror-lens combination (Andrews et al 1958). This system was modified by adding a metal plate in front of the fluorescent screen (Benner et al 1962), and developed and refined years later by several groups (Leong 1986, Shalev et al 1989, Munro et al 1987, 1988, 1990a, 1990b, Ezz et al 1991, Swindell et al 1991, Racliffe et al 1993, Jaffray et al 1995a, 1995b, Bissonnette et al 1994, 1997a, 1997b, Drake et al 2000). The commercialization of camera based EPIDs started in the late 1980s. An alternative two-dimensional optical technology for electronic portal imaging based on thin film electronics of the sort used in active matrix liquid crystal displays was developed (Antonuk et al 1991a, 1992a, 1998a, 1998b). This system so called amorphous-silicon EPID (a-SI EPID) or flat-panel imager, consisted of a phosphorus screen and a thin-film transistor diode array. In addition to these two-dimensional optical systems, another interesting optical system approach involved a

one-dimensional detector array scanned across the field of view (Morton and Swindell 1987, Morton 1988, Morton et al 1991) that offered high quality images. A new version of this type of EPID that allows increased light yield, and a better signal-to-noise ratio, was developed years later (Spies et al 2000, Evans et al 2000) [3][25].

While the bulk of efforts to develop optical EPIDs have been directed toward two-dimensional systems, this was not the case for non-optical systems. The first non-optical system developed consisted of a scanning linear array of silicon diodes (Taborsky et al 1982, Lam et al 1986, 1987) and photovoltaic diodes (Entine et al 1992, 1993). While the first device was known as a scanning liquid-filled ionization chamber, the second device was known as a scintillation crystal-photodiode. Another non-optical system developed was based on a two-dimensional matrix ionization chamber (Van Herk and Meertens 1987, Van Herk 1991, Van Herk et al 1992, Merteens et al 1985, 1990). This system was commercially available since 1990 and, like the camera-based EPID systems using a metal plate/phosphor screen, produced images with significant amounts of clinically useful information. More recently, two other novel non-optical approaches for EPID design have been explored: a one-dimensional scanning system employing the kinestatic charge detection principle (DiBianca et al 1997, Samant et al 1999), and a dual-energy two-dimensional imager consisting of multiple gas-electron multiplier detectors (Brahme et al 2000, Ostling et al 2000, Iacobaeus et al 2001) [3][25].

Basically, EPIDs can be of four different types: scanning liquid-filled ionization chamber, scintillation crystal-photodiode, camera-based EPID, and amorphous-silicon EPID (a-SI EPID) or flat-panel imager.

The type of EPID most widely used and available today is the amorphous-silicon EPID (a-Si EPID) or flat-panel imager (Antonuk et al 1995, 1998). The panel consists in an X-ray converter that is optically coupled to a camera by means of a mirror and a lens, a light detector, and an electronic acquisition system for receiving and processing the resulting digital image. The converter consists in a flat metal plane, which serves to convert incident primary X-rays into high energy electrons, as well as to block low energy scattered radiation, and a gadolinium oxysulfide phosphor screen which serves to convert primary X-rays into high energy electrons, and transforms a fraction of the energy of the high energy electrons passing through it into light. Some of the light diffuses through the screen, exiting on the mirror side. Then, a fraction of this emerging light is captured by the camera and lens and transformed into a video signal that is sent to other hardware for digitization, processing, display and archiving. The reason a-Si detectors have become increasingly popular for portal imaging is because they have relatively higher detector quantum efficiency than, for example, the liquid filled ionization chamber EPID, requiring less patient dose for the same portal image [3][21].

Basically, EPID is a heavy piece of hardware mounted on a support arm that allows vertical, lateral, and longitudinal translations, as well as a pitch rotation.

2.3.2 PDI (Portal Dose Image)

A portal dose image (PDI) is acquired with the radiation obtained from the radiotherapy treatment, and it consists in a 2D distribution of the photon transmission behind a patient during the external beam radiotherapy. Initially, portal images were obtained using films, and used to verify the patient position once they show the irradiated area. However, as the time passed by, films were replaced by EPIDs, once EPIDs allow the acquisition of digital images with high precision. Nowadays, the use of portal images has been extended to treatment verification.

2.3.3 Dosimetric Calibration of an a-Si EPID

The standard calibration of EPID requires the acquisition of a dark-field image, a flood-field image and a defective pixel map to achieve a more uniform EPID response. The dark-field image is the average of several frames acquired without radiation and, therefore, it is the same for all treatment energies. The flood-field image is the average of several frames acquired by irradiating EPID with an open uniform field, large enough to cover the entire active matrix. The defective pixel map identifies all the nonresponding pixels to assign them the mean value of the neighboring pixels [21].

First, to correct individual pixel background signals, the dark-field image is obtained (the same for all treatment energies). Then, for each treatment energy, a flood-field image is acquired to normalize each individual pixel response, correcting differences in pixel sensitivities. Finally, to enhance the image quality, a defective pixel map is acquired. It is important to note that, before to be stored and displayed, each frame acquired by EPID is automatically darkfield and flood-field corrected by the image acquisition system. Therefore, each portal image (PIRaw) is subtracted by the dark-field (DF) image and divided by the normalized flood-field (FF) image, which is also dark-field corrected, and multiplied by a mean value of the normalized flood-field image (FFMean) according with the next equation,

$$\boldsymbol{PI_{corrected}(x,y) = \frac{PI(x,y) - DF(x,y)}{FF(x,y)} \times FF_{mean}} \textbf{ (Equation 2.1)}$$

Ideally, for dosimetry purposes the FF image should be perfectly flat. However, since the FF image is generated from an open photon beam, it exhibits the characteristics horns caused by the flattening filter. Therefore, the FF image not only corrects pixel-to-pixel sensitivity variation or off-axis differential energy response, but also removes the beam profile present in the acquired portal image causing spatial distortions in the fluence distribution. For this reason, a previously calculated or measured (with film or ionization chamber in water) beam profile (BP) is used to restore the initial beam profile of the acquired portal image, so

$$PI_{corrected}(x,y) = \frac{PI(x,y) - DF(x,y)}{FF(x,y)} \times FF_{mean} \times BP \textbf{ (Equation 2.2)}$$

To perform dosimetric calibration of EPID, two different approaches have been adopted: prediction of the grayscale pixel value or conversion of grayscale pixel value to dose or fluence value. The first one

models the EPID response by Monte Carlo simulation or empirical models and, for this reason, an accurate and detailed knowledge regarding EPID composition is required. In turn, the second approach converts the portal image acquired by EPID into a portal dose image applying empirical models based on measurements in water with a calibrated detector, usually an ionisation chamber. In general, converting grayscale values to dose or fluence is simpler and faster than a modulation of the EPID response and, therefore, more suited for clinical implementation.

2.3.4 Methods of EPID Dosimetry

There is no clear consensus in the literature on the definition of various procedures and methods related to EPID dosimetry. However, below, there is a definition of various terms as used in this thesis.

Verification procedures can be classified according to whether they are performed during treatment time (i.e. with the patient), or outside of treatment time (i.e. without the patient). Thus, we can have:

- Pre-treatment verification (without the patient), where the whole or part of the intended treatment plan is compared with measurements of corresponding radiation beams delivered by the linear accelerator outside patient treatment time, i.e., with open fields (without anything) or a phantom;
- Treatment verification (with the patient), where all or part of the planned dose is compared with the delivered dose distribution based on measurements acquired during patient treatment time [3].

Dosimetry methods, independent of the type of detector used, can be grouped according to whether beams have passed through an attenuating medium, or whether the dose is reconstructed inside a phantom or patient. We can have:

- Non-transmission (or non-transit) dosimetry (without an attenuating medium), which consists in the determination of the dose in the detector, patient or phantom, or determination of the incident energy fluence, based on measurements without an attenuating medium between the source and the detector, i.e., phantom or patient;
- Transmission (or transit) dosimetry (with an attenuating medium), which is based in the determination of the dose at the position of the detector, patient or phantom, or determination of the incident energy fluence, based on radiation transmitted through the patient or phantom;
- In-phantom dosimetry (inside a phantom), which consists in the measurement or determination of the dose inside a phantom (rarely performed with EPIDs but included for completeness). This can be the dose at points, lines, planes, or volumes within the phantom;
- *In vivo* dosimetry (inside a patient), that relies on measurement or determination of the dose inside the patient. Measurements performed during treatment can be performed invasively, i.e., inside the patient, or non-invasively, i.e., at some distance from the patient, whereby the *in vivo* dose at the point of interest is obtained by extrapolation [3].

2.3.5 Pre-treatment Verification vs *In Vivo* Dosimetry

Portal dose images are frequently used for pre-treatment verification of IMRT fields, and *in vivo* dosimetry. As said before, in the first case, the goal is to verify the accuracy of dose delivery in a phantom prior to the first radiotherapy session and, therefore, to detect errors before the first fraction. For that, an

algorithm based on pencil beam kernels is used to calculate dose images that will reflect the intended transmission distributions at the large focus-EPID distance in absence of a patient. In the case of *in vivo* dosimetry, the goal is to verify the dose actually delivered to a patient during treatment time [23].

The main advantages of *in vivo* dosimetry over pre-treatment verification include high resolution 2D digital images available immediately after irradiation, very little additional clinical time, containing both dose and anatomical information, providing a check and documentation of the actual patient treatment (since measurements are acquired during treatment time), and the fact that the panel is already fixed to the LINAC.

Either pre-treatment or *in vivo* dosimetry can be done using two different approaches: forward approach and backward approach. In the first approach (forward approach), the measured portal image is compared to a predicted dose, or photon fluence, at the plane of the EPID calculated with the treatment planning system (TPS), or by an independent dose calculation algorithm, while in the second approach (backward approach), a portal image is used to reconstruct the dose within the patient or phantom. This last method is more complicated but makes it possible to directly compare the calculated with the delivered dose distribution in the patient or phantom. A scheme illustrating the two different approaches can be seen in the figure below, **Figure 2.7**.

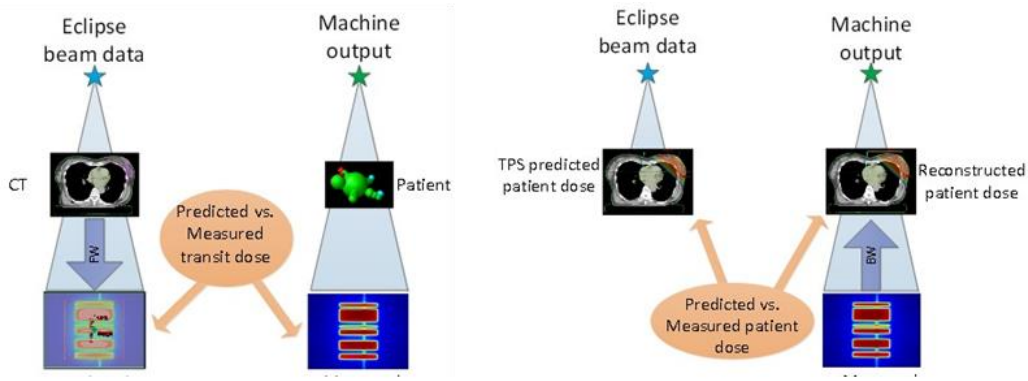

Figure 2.7. The (a) forward and (b) backward approach for pre-treatment and *in vivo* dosimetry. Adapted from [25].

At the Radiotherapy Department of Champalimaud Foundation, there is forward projection EPD with an algorithm to calculate the dose at the level of EPID that is only used with plans that doesn't have FFF (flattening filter free), and there is also back projection EPD.

2.3.6 Back Projection Methods

As mentioned before, portal dose images are not only useful to verify if the planned portal dose is identical to the measured portal dose, but they can also be used to make a full 3D reconstruction of the actual dose delivered to a patient using back projection methods.

Back projection methods relate the primary portal dose with the dose effectively delivered to the patient. Therefore, is necessary to separate the primary portal dose, related with the radiologic thickness of

the path crossed by the photons in the patient, from the patient's dispersed dose in EPID position, which comes from all the patient's irradiated parts. In this way, a theoretical back projection method will describe the relationship between three types of data - 2 PDIs, one with and the other one without any object (i.e., phantom, if it is pre-treatment, or patient, if it is *in vivo*), and the radiologic thickness of the path crossed by the phantoms in the object - and must be able to extract the primary portal dose from a PDI measured during the treatment. Note that the radiologic thickness is related with the primary portal dose through the attenuation coefficient along the X-ray lines, and the prediction of a portal dose image is based in the assumption that the radiologic mean plan matches the isocenter plan.

To sum up, back projection methods allow:

- Dosimetric calibration to establish the dose-response relationship by relating EPID pixel values to dose values at the position of the imager;
- Determination of the parameters for the back projection to enable the conversion from the dose at EPID position to the dose inside the patient or phantom. This is done by applying correction procedures for the scatter component of the dose within EPID and the scatter from the patient or photon to EPID;
- Obtainment of the total dose at a specific point in the patient or phantom, taking in account the scatter component within the patient or phantom in combination with the attenuation beam.

2.3.7 State of the Art

Pre-Treatment Dosimetry

Talamonti et. al [32], used a commercial amorphous silicon electronic portal imaging device (EPID) to investigate its potential in the field of pre-treatment verifications of step and shoot, intensity modulated radiation therapy (IMRT), 6 MV photon beams. The a-Si EPID demonstrated a good linearity with dose (within 2 % from 1 MU), which represent a pre-requisite for the application in IMRT. Ma et al. [33] employed a fast beam imaging system (BIS, Wellhöfer, Germany), and compared measured images with reference images generated from the MLC leaf sequencing files. Gross errors, such as flipped reference images, as well as positional errors of 0.5 mm in the leaf motion, were readily detected by the presented procedure. Curtin-Savard et al. [34] reported on the use of a liquid-filled portal imager for the dosimetric verification of step-and-shoot delivery by acquiring a portal image for every subfield of the leaf sequence. After their calibration, the images were multiplied by their respective associated monitor unit (MU) settings, and summed to produce a planar distribution at the measurement depth in a phantom. These distributions were then compared with dose distributions predicted by the TPS. Pasma et al. [35] reported on the use of a CCD-camera based fluoroscopic EPID for pre-treatment verification of intensity modulated beams produced with a DMLC. Due to the high data acquisition rate of these cameras, and their capability to measure simultaneously in all points of the treatment field, integrated images could be obtained. These images were then converted into two-dimensional dose distributions, and compared with the calculated dose distributions. For the reported profiles, the agreement between predictions and EPID measurements, and between ionization chamber measurements and EPID measurements, was within 2 % (1 SD). Chang et al. [36] developed a quality assurance procedure to assess the intensity profile, and dosimetry for intensity

modulated treatments fields, using a liquid-filled portal imaging device (PortalVision Mk1, Varian Medical Systems, Palo Alto, CA). To overcome the limited acquisition rate of their detector (5 s/image for the fast acquisition mode), the leaf speed was intentionally slowed down by drastically increasing the amount of MUs (which increased the treatment verification time, enabled the detection of any error influenced by the speed of the leaves and, therefore, led to an incomplete verification). Esch et. al [37] investigated the use of a commercially available, liquid-filled EPID (PortalVision Mk2, Varian Medical Systems) for dosimetric verification of intensity modulated beam profiles, delivered with a dynamic MLC, and concluded that accurate dosimetric images could be obtained. The dosimetric accuracy of the measured dose distribution was ~2 % with respect to film and ion chamber measurements, and, when comparing the acquired and expected distributions, an overall agreement of 3 % was obtained. Years later, Esch et. al [21], investigated the basic dosimetric characteristics of an aSi portal imager (aS500, Varian Medical Systems), using an acquisition mode especially developed for portal dose (PD) integration during delivery of a static or dynamic- radiation field. Absolute rather than relative dose prediction was applied, and the PD image prediction was compared to the corresponding acquisition for several clinical IMRT fields by means of the gamma evaluation method. They concluded that, although the dose deposition behavior in the portal image detector was not equivalent to the dose to water measurements, it was reproducible and self-consistent, lending itself to quality assurance measurements. Gamma evaluations of the predicted versus measured portal dose distribution were within the pre-defined acceptance criteria for all clinical IMRT fields (i.e. allowed a dose difference of 3 % of the local field dose in combination with a distance to agreement of 3mm).

In vivo Dosimetry

Nijsten et. al [38], used a calibrated camera-based EPID to measure the central field dose, which was then compared with a dose prediction at EPID level. For transit dosimetry, dose data was calculated using patient transmission and scatter, and compared with measured values. Furthermore, measured transit dose data was back-projected to an *in vivo* dose value at 5 cm depth in water (D5), and directly compared with D5 from the treatment planning system. The results showed that pre-treatment measurements had a mean dose difference per treatment session of 0.0 ± 1.7 % (1 SD), and *in vivo* measurements had a mean transit and a D5 dose differences of -0.7 ± 5.2 % (1 SD) and -0.3 ± 5.6 % (1 SD) per treatment session, respectively. Pasma et. al [39], proposed a method for *in vivo* verification of the MU calculation of the treatment beams. The method was based on comparison of the intended on-axis patient dose at 5 cm depth for each treatment beam, D5, with D5 as derived from the portal dose Dp measured with an EPID. The results obtained confirmed the accuracy of the method in verifying the MU calculation of an X- ray beam, and in discriminating errors that were due to changes in patient anatomy related to appearance or disappearance of gas pockets in the rectum, and errors due to a deviating cGy/MU value. Piermattei et. al [40], developed a method for the *in vivo* determination of the isocenter dose, Diso, and mid-plane dose, Dm, using the transmitted signal St measured by 25 central pixels of an aSi-based EPID. The method had been applied to check the conformal radiotherapy of pelvic tumors, and supplied accurate *in vivo* dosimetry, avoiding many of the disadvantages associated with the use of two diode detectors (at the entrance and exit of the patient) as their periodic recalibration and their positioning. The agreement between the *in vivo* dosimetry and stated doses at the isocenter point were within 3 %. One year later, for the first time,

Piermattei et. al [41], applied the method developed to brain and thorax irradiations using a transit signal St. The transit signal St was measured along the beam central axis by a small air ion-chamber, positioned on EPID, or by a last generation EPID. The method, that used correlation functions determined by the ratios between St and Dm measured in standard water-equivalent phantoms, was applied to determine Diso even in the presence of asymmetric inhomogeneities. The results showed that the tolerance/action levels for every radiotherapy fraction were 4 % and 5 % for the brain (symmetric inhomogeneities) and thorax/pelvic (asymmetric inhomogeneities) irradiations, respectively. In this way, the variations between the total measured and prescribed doses at the isocenter point in five fractions, were well within 2 % for the brain treatment, and 4 % for thorax/pelvic treatments.

2.4 Dose Verification

In pre-treatment patient-specific QA of IMRT and VMAT plans, dose verification is needed to avoid underdose of the target volume or overdose of the normal tissues. Thus, different methods that allow the efficient and accurate comparison between the calculated and the measure dose distribution, have been developed and used in clinical practice.

2.4.1 Profile Comparison

One method that is very useful when evaluating local deviations between dose distributions is the profile comparison. This consists in plotting, against each other, the evaluated and reference dose distributions profiles in the X, Y, or diagonal directions, to be visually compared.

2.4.2 Distance-to-Agreement

The distance-to-agreement (DTA) consists in measuring the spatial difference between a point in the reference dose distribution, $\overrightarrow{r_r}$, and the closest point with the same dose value in the evaluated dose distribution, $\overrightarrow{r_e}$, such that,

$$\Gamma(\overrightarrow{r_r}, \overrightarrow{r_e}) = min|\overrightarrow{r_e} - \overrightarrow{r_r}| \quad \textbf{(Equation 2.3)}$$

Usually, a threshold value of Δd, typically $\Delta d = 3mm$, is considered as acceptance criteria in a way that if the DTA at the evaluated point $\overrightarrow{r_e}$ is higher than Δd, the DTA criterion fails, otherwise, if the DTA at the evaluated point $\overrightarrow{r_e}$ is lower than Δd, the DTA criterion passes [28].

2.4.3 Gamma Evaluation

Nowadays, the gold standard method for the evaluation of comparisons between measured and calculated absorbed dose distributions is the so-called gamma evaluation method.

The gamma method was designed by Low et al [28] to compare two dose distributions. In this, one dose distribution is used as reference (Dr), while the other is used for evaluation (Dc), taking in account the dose and spatial differences between them. Thus, the gamma evaluation method is a tool that allows the comparison of dose distributions on a quantitative manner by combining dose difference (DD) and distance-to-agreement (DTA) criteria to determine if the compared dose points pass or fail the dose distribution comparison test.

The acceptance criterion is denoted by ΔDM (measured in %) for DD, and by ΔdM (measured in mm) for DTA, and is usually 3 %, 3 mm (once IMRT dose distributions often dose gradients of close to 3%/3 mm). The evaluation is performed for each point in the reference dose distribution, $\overrightarrow{r_r}$, to find the most similar point in the evaluated dose distribution, $\overrightarrow{r_e}$, and provides a numerical quality index, referred to as gamma value or gamma index. The gamma index is basically a measure of agreement or disagreement in regions that pass or fail the acceptance criteria, respectively, reflecting the calculation quality in these regions [29].

For 2D dose distributions, the gamma method is denoted by an ellipsoid surface (**Figure 2.8**) representing the acceptance criteria for dose and spatial tolerance with the center located at $\overrightarrow{r_r}$,

$$\Gamma(\overrightarrow{r_r},\overrightarrow{r_e}) = \sqrt{\frac{r^2(\overrightarrow{r_r},\overrightarrow{r_e})}{\Delta d_M^2} + \frac{\delta^2(\overrightarrow{r_r},\overrightarrow{r_e})}{\Delta D_M^2}} \quad \textbf{(Equation 2.4)}$$

where $r^2(\overrightarrow{r_r},\overrightarrow{r_e})$ is the spatial distance between the evaluated point, $\overrightarrow{r_e}$, and the reference point, $\overrightarrow{r_r}$, i.e., $r^2(\overrightarrow{r_r},\overrightarrow{r_e}) = |\overrightarrow{r_e} - \overrightarrow{r_r}|$, and $\delta^2(\overrightarrow{r_r},\overrightarrow{r_e})$ is the dose difference between the evaluated dose D_e, at position $\overrightarrow{r_e}$, and the reference dose D_r, at position $\overrightarrow{r_r}$, i.e., $\delta^2(\overrightarrow{r_r},\overrightarrow{r_e}) = |D_e(\overrightarrow{r_e}) - D_r(\overrightarrow{r_r})|$. The gamma index is then calculated by finding the minimum value of $\Gamma(\overrightarrow{r_r},\overrightarrow{r_e})$ so that,

$$\gamma(\overrightarrow{r_r}) = \min\{\Gamma(\overrightarrow{r_r},\overrightarrow{r_e})\}, \forall\ \{\overrightarrow{r_e}\} \quad \textbf{(Equation 2.5)}$$

Finally, for the compared distribution to match, the gamma value for the reference dose at position $\overrightarrow{r_r}$ must be equal or smaller than 1. Otherwise, i.e., if $\gamma(\overrightarrow{r_r}) > 1$, we can conclude that the evaluated point $\overrightarrow{r_e}$ is not within the specified acceptance criterion [29].

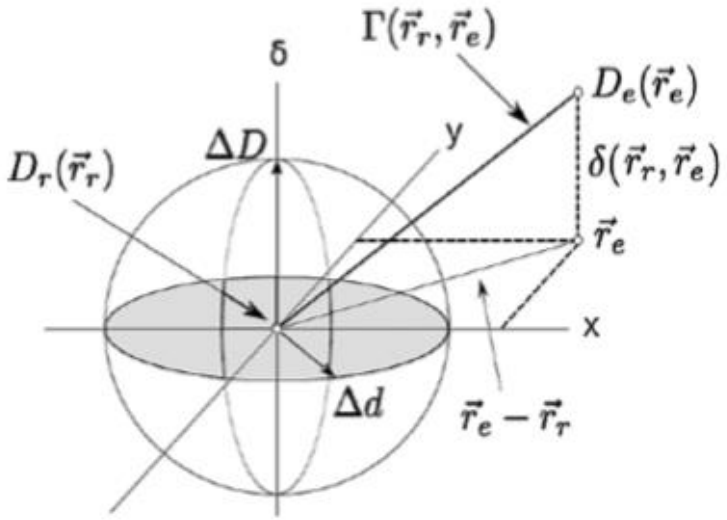

Figure 2.8. Geometric representation of the theoretical concept of the gamma evaluation method for 2D dose distributions. In this example, the evaluated point, $\vec{r_e}$, fails the criterion. Retrieved from [29].

The most common approach is based on the use of a global criterion for DD, where ΔD_M is constant for all points evaluated and calculated regarding the maximum dose. When instead of using a global criterion for DD, a local criterion for DD is used (ΔD_M not constant and calculated regarding the dose at the reference point), a stricter constraint should be use.

It is important to note that, due to the unavoidable uncertainties of absorbed dose measurements and detector positioning, some points in the gamma evaluation may fail the test criteria even if there is no true deviation and, therefore, a certain failure rate should be tolerated.

Compared to dose difference, the gamma evaluation is less sensitive to spatial deviation to the imager from the optimal position. For this reason, gamma image is the main source for statistic evaluation but it is not suited for alignment because of the principle of the underlying algorithm, which, as mentioned before, allows a certain spatial deviation. However, it can be used for virtual inspection of the degree of agreement between predicted and measured dose after alignment.

In the case of Portal Dosimetry (portal dose image prediction) software, i.e., the Varian software available for portal dosimetry, when applying the gamma evaluation method, we obtain a measure called gamma passing rate – a value between 0 % and 100 % - which will reflect the success/failure of the irradiation plan. In other words, the magnitude of the gamma passing rate will correspond to the dose discrepancy between the planned dose and the actual delivered dose for a given plan.

CHAPTER 3. MATERIALS AND METHODS

As said previously, in the Radiotherapy Department of the of the Champalimaud Foundation, there are two different Varian LINAC, TrueBeam™ and Edge™ (Varian Medical Systems, Palo Alto, CA, USA), that have different a-Si EPIDs incorporated in the retractable robotic arm – aS1000 and aS1200, respectively, with different characteristics (Erro! A origem da referência não foi encontrada.). To perform pre-treatment dosimetry for both IMRT and VMAT plans, Varian had developed a Portal Dose Image Prediction Algorithm and a Portal Dosimetry software inside the ARIA® interface.

	TrueBeam™	**Edge™**
PortalVision	aS1000	aS1200
Active Matrix Area	30 cm x 40 cm	43 cm x 43 cm
Pixel Number	1024 pixel x 768 pixel	1280 pixel x 1280 pixel
Pixel Size	0.39 mm x 0.39 mm	0.34 mm x 0.34 mm
Maximum Frame Rate	10 frames per second	25 frames per second
Maximum Dose Rate	1000 MU/min	5000 MU/min

Table 3.1. Characteristics of the different Varian LINAC EPIDs.

In the next figures, **Figure 3.1** and **Figure 3.2**, we can see the TrueBeam™ and Edge™ LINAC, without and with EPID opened, respectively.

(a) (b)

Figure 3.1. TrueBeam™ LINAC (a) without and (b) with EPID (red arrow) opened.

Figure 3.2. Edge™ System (a) without and (b) with EPID (red arrow) opened.

In **Figure 3.3**, we can see ArcCHECK, from both sides, as well as ArcCHECK mounted on the Edge™ LINAC.

Figure 3.3. ArcCHECK viewed from (a) the front part and from (b) the back part, and (c) mounted on the LINAC. Note that in order to place ArcCHECK correctly, we have to align the lasers with ArcCHECK marks, and then with the light field.

3.1 Varian Portal Dosimetry Solution

The Varian Portal Dosimetry solution includes an EPID, a Portal Image Dose Prediction (PDIP) algorithm, and a Portal Dosimetry software. The EPID can be one of three a-Si models: PortalVision aS500, aS1000 or aS1200. The PDIP algorithm is a dedicated 2D-algorithm to predict the portal dose image that will be the first clinical VMAT verification. Finally, the Portal Dosimetry software allows the comparison (gamma evaluation) between predicted and portal dose images acquired by EPID (see **Figure 3.4)**.

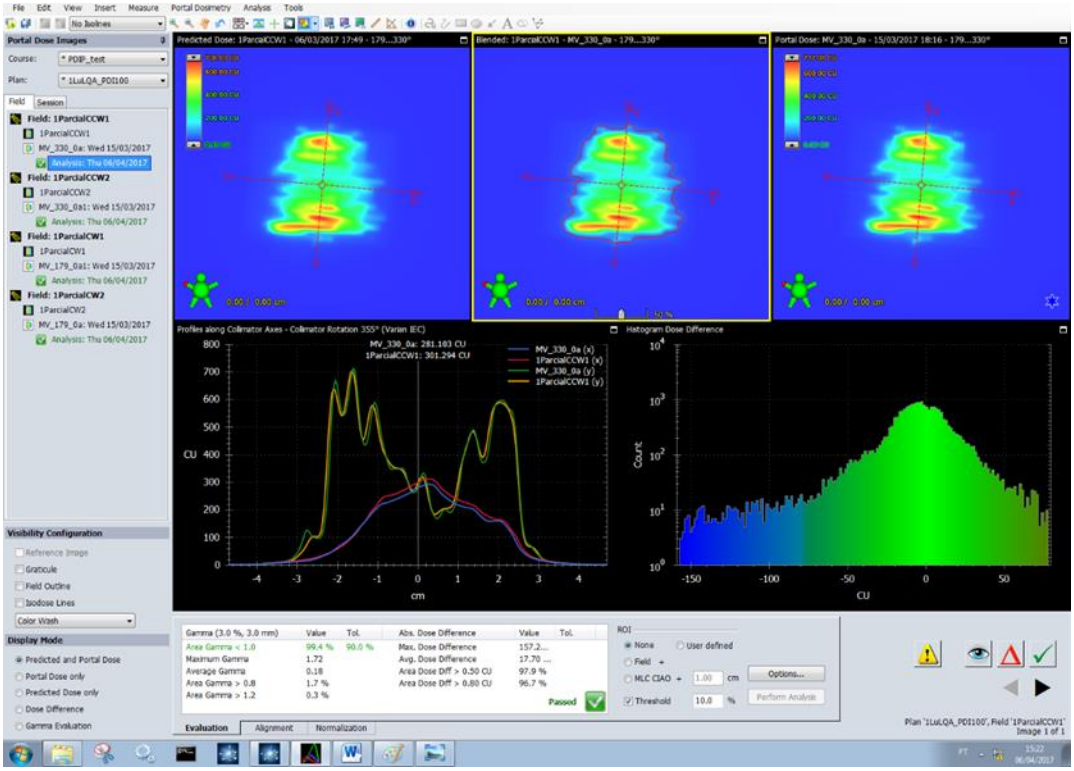

Figure 3.4. Portal Dosimetry workspace.

Regarding the Portal Dosimetry workspace shown in **Figure 3.4**, we can see the portal dose image acquired with EPID (in the upper right side) and the correspondent portal dose image predicted by the PDIP algorithm (in the upper left side). The acquired and the predicted portal dose images are automatically blended resulting in the portal dose image sown in the center. After the analysis, the results appear in the white box, and the profiles along collimator x and y for both images, as well as a dose difference histogram, are displayed. In this case, the acquired portal dose image is nearly indistinguishable from the correspondent predicted dose, resulting in a gamma passing rate of 99.4 % for the 3 %/3 mm criterion. It is important to note that the evaluated area is the complete irradiation area outline (CIAO).

In the next figures, **Figure 3.5** and **Figure 3.6**, we can see in more detail the profiles along collimator x and y for another acquired and predicted portal dose images, as well as a gamma evaluation histogram of the composite portal dose image (result of the combination of the portal dose images obtained for each arc of the plan), respectively.

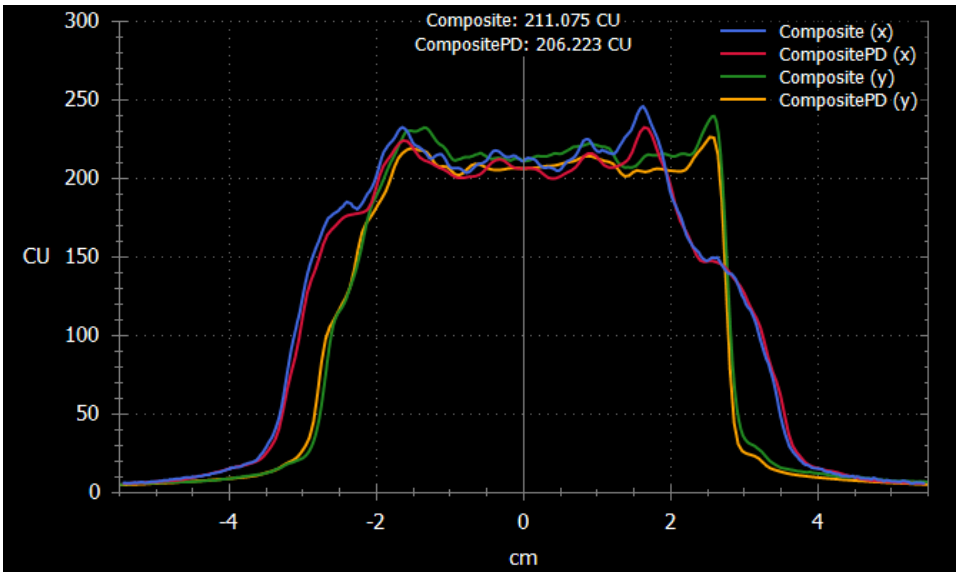

Figure 3.5. Profiles along collimator x (blue and red lines) and y (green and yellow lines) for acquired (blue and green lines) and predicted (red and yellow lines) portal dose images.

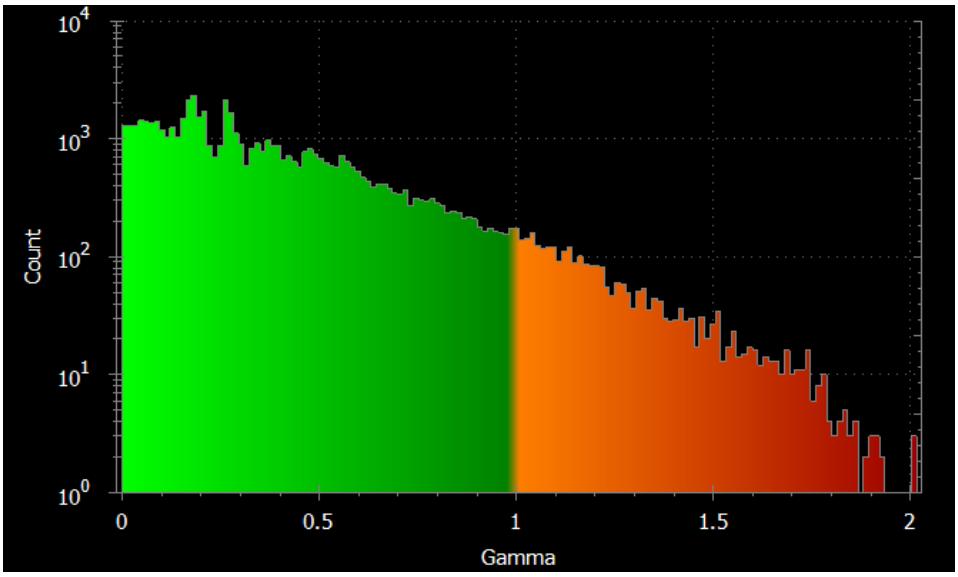

Figure 3.6. Gamma evaluation histogram of the composite portal dose image.

Regarding the main purpose of this work – replace ArcCHECK QA measurements and bring into the clinic the routinely use of EPID to perform QA measurements – different studies were conducted:

- **Study A**: On the TrueBeam™ LINAC, the performance of the Portal Dosimetry solution for pre-treatment patient-specific QA of IMRT and VMAT plans was compared with ArcCHECK;

- **Study B**: On the Edge™ LINAC, the performance of the Portal Dosimetry solution for pre-treatment patient-specific QA of IMRT and VMAT plans was compared with the performance of the same solution on the TrueBeam™ LINAC;
- **Study C**: On the Edge™ LINAC, the performance of the Portal Dosimetry solution for pre-treatment patient-specific QA of IMRT and VMAT plans was compared with ArcCHECK;
- **Study D**: On the Edge™ LINAC, errors were introduced in the patient plans in order to study the sensitivity of EPID during pre-treatment patient-specific QA
- **Study E**: On the Edge™ LINAC, errors were introduced in the patient plans to study the sensitivity of ArcCHECK during pre-treatment patient-specific QA, and the sensitivity of both ArcCHECK and EPID systems was compared;
- **Study F**: Finally, on the Edge™ LINAC, a software was developed in order to export the patient plans with errors into the ARIA® interface and evaluate the effects of the different types of error in the organs at risk, to see whether clinically relevant errors would be detected with EPID/ArcCHECK.

All the measurements, in each one of the studies mentioned before, were performed with non-transit dosimetry at EPID level (EPID at 100 cm), according to the specifications of the EPID attached to each Varian LINAC in the Radiotherapy Department of Champalimaud Foundation (TrueBeam™ and Edge™ systems).

3.2 Data Sets

3.2.1 Study A

In the first study, Study A, the aim was to compare the gamma passing rates values obtained when performing pre-treatment patient-specific QA with ArcCHECK and with EPID, on the TrueBeam™ LINAC, in order to prove that EPID is as good, or even better than ArcCHECK. For that, 163 anonymized 6 MV IMRT and VMAT patient plans were irradiated on the TrueBeam™ LINAC (from September 2016 to November 2016) for both ArcCHECK and EPID systems (see **Table 3.2**).

In an initial phase, the patients were selected and previously planned using Eclipse. Once planned and scheduled, each patient plan was tested a priori on the TrueBeam™ LINAC available at the Radiotherapy Department of the Champalimaud Foundation. Finally, after the irradiation, using the Portal Dosimetry software (version 10), the portal imagens obtained from the irradiation were analysed and compared with the predictions, in order to make a comparison between the prescribed dose and the dose actually given, as well as a gamma passing rate evaluation. The results obtained with the EPID system were then compared with the ones obtained previously with ArcCHECK. It is important to notice that, to avoid bias, we have included both rejected and accepted patient plans after performing pre-treatment patient-specific QA with ArcCHECK, i.e., both patient plans with a gamma passing rate below and above 90 %, respectively (when we have 90 % or more of the points with gamma < 1, we plan is accepted; otherwise, the plan is rejected). If we had only considered patient plans accepted after performing pre-treatment patient-

specific QA with ArcCHECK, we would be conditioning the results once we would be only considering the ones that had a good gamma passing rate and, therefore, the ones that probably had also a good gamma passing rate after performing pre-treatment patient-specific QA with EPID. In the analysis of the results, a gamma criterion of 3 %/3 mm was used, and two thresholds of 90 % and 95 % were considered.

Table 3.2. Information correspondent to the treatment course and dose per fraction for each one of the 163 patients included in the first study, Study A.

# Patients	Treatment Course		Dose per Fraction (Gy)
50	Thorax	(6)	2.7
		(43)	3.2
		(1)	3.4
112	Pelvis	(1)	1.8
		(10)	2.25
		(101)	2.5
1	Member		1.8

3.2.2 Study B

The second study, Study B, which aimed to compare the average gamma values, as well as the average dose difference values, obtained when performing pre-treatment patient-specific QA with EPID, for two different LINACs (TrueBeam™ LINAC and Edge™ LINAC), included 16 anonymized 6 MV IMRT and VMAT prostate and breast patient plans (irradiated on October 2016). The analysis software used (Portal Dosimetry version 10) was the same in both cases (see Erro! A origem da referência não foi encontrada.**)**.

The method used in this study was the same as the one mentioned for the Study A with the difference that, this time, each patient plan was irradiated on both TrueBeam™ and Edge™ LINAC in order to compare the two LINACs used. In the analysis of the results, a gamma criterion of 3 %/3 mm was used.

Table 3.3. Information correspondent to the treatment course and dose per fraction for each one of the 16 patients included in the second study, Study B.

# Patients	Treatment Course		Dose per Fraction (Gy)
6	Thorax	(2)	2.7
		(3)	3.2
		(1)	3.4
10	Pelvis		2.25

3.2.3 Study C

The aim of the third study, Study C, was, like the Study A, to compare the gamma passing rates values obtained when performing pre-treatment patient-specific QA with ArcCHECK and with EPID, on the Edge™ LINAC, in order to prove that EPID is as good, or even better, than ArcCHECK. For that, 91 anonymized IMRT and VMAT patient plans were irradiated on the Edge™ LINAC (from December 2017 to February 2017). Unlike the previous studies, this study included patient plans with both 6 MV and FFF beams (see **Table 3.4**).

The method used for this study was the same as the one described in the previous studies, with the difference that, while in Study A, the thorax patients were mainly breast patients, in this study, the thorax patients were mainly lung patients. In the analysis of the results, a gamma criterion of 3 %/3 mm was used, and two thresholds of 90 % and 95 % were considered.

Table 3.4. Information correspondent to the treatment course and dose per fraction for each one of the 91 patients included in the third study, Study C.

# Patients	Treatment Course		Dose per Fraction (Gy)
32	Thorax	(1)	7
		(9)	8
		(3)	9
		(2)	22
		(16)	24
		(1)	26
36	Pelvis	(3)	5
		(1)	6.5
		(1)	6.7
		(3)	7
		(1)	7.5
		(5)	8
		(4)	9
		(1)	10
		(17)	24
13	Abdomen	(3)	8
		(1)	10
		(1)	18
		(8)	24
2	Member		8
8	Brain	(1)	4
		(1)	7
		(1)	10

		(1)	18
		(4)	24
1	Head & Neck		7

3.2.4 Study D

In the fourth study, Study D, the aim was to introduce errors in the XML files (plain text files that describe the transportation, structure, and storage of data) with the patient plans to test the sensitivity of EPID incorporated on the Edge™ LINAC, i.e., in order to verify if there is any relationship between the values of the average gamma and the magnitude of the error introduced. Four different types of error were introduced - errors in the MUs, errors in the MLC position (random and systematic), and errors in the collimator angle. For that, 4 anonymized FFF IMRT and VMAT patient plans were irradiated (on November 2016) on the Edge™ LINAC (see **Table 3.5**).

Unlike the three previous studies, in an initial phase, the patient plans were converted in XML files. Then, using the ReadDCMPlan software, different types of error were introduced for the four different patients. Once introduced the errors in the XML files, the files were transferred into the Edge™ LINAC, to irradiate the plans. Finally, after the irradiation, the portal images obtained were stored in the data base, and downloaded in the Varian Citrix. In this platform, using the Portal Dosimetry software (version 13) and converting the images to DICOM files according to each magnitude of error introduced, for each arc, and for each patient, the portal images were analysed and compared with the ones from the CT, in order to make a comparison between the prescribed dose and the dose actually given, as well as an average gamma evaluation. In the analysis of the results, a gamma criterion of 3 %/3 mm was used.

Table 3.5. Information correspondent to the treatment course and dose per fraction for each one of the 4 patients included in the fourth study, Study D.

# Patients	Treatment Course		Dose per Fraction (Gy)
1	Pelvis		2
2	Brain	(1)	10
		(1)	18
1	Head & Neck		46

3.2.5 Study E

The fifth study, Study E, aimed introduce errors in the XML files in order to test the sensitivity of both EPID and ArcCHECK. Four different types of error were introduced - errors in the MUs, errors in the MLC position (random and systematic), and errors in the collimator angle – in four different chosen patients. This fifth study included 7 anonymized FFF IMRT and VMAT patient plans that were irradiated (on May 2017) on the Edge™ LINAC (see **Table 3.6**).

Since we were testing the sensitivity of the ArcCHECK system as well, we had to introduce errors in the patient plans. The way we found to do so included, in an initial phase, converting the patient plans in XML files. Then, using the ReadDCMPlan software, different types of error were introduced for the three different patients. Once introduced the errors in the XML files, the files were converted to a DICOM format to import them into the ARIA® interface. After this, the files were transferred into the Edge™ LINAC, to be possible to irradiate the plans. Finally, after the irradiation, the portal images obtained were stored in the data base, and downloaded in the Varian Citrix. In this, using the Portal Dosimetry software (version 13) and converting the images to DICOM files according to each magnitude of error introduced, for each arc, and for each patient, the portal images were analysed and compared with the prescribed, in order to make a comparison between the prescribed dose and the dose actually given, as well as an average gamma evaluation. In the analysis of the results, a gamma criterion of 3 %/3 mm was used.

Table 3.6. Information correspondent to the treatment course and dose per fraction for each one of the 7 patients included in the fifth study, Study E.

# Patients	Treatment Course		Dose per Fraction (Gy)
5	Thorax	(1)	2.25
		(1)	20
		(2)	24
		(1)	27
2	Pelvis	(1)	2
		(1)	5

3.2.6 Study F

Finally, the aim of the sixth and last study, Study F, was to introduce errors in the XML files and export the plans with errors into the ARIA® interface in order to compare the plans with errors with the ones without errors and, therefore, verify the effect of the errors in the organs at risk. For that, 1 anonymized FFF IMRT patient plan was irradiated (on June 2016) on the Edge™ LINAC (see **Table 3.7**).

The procedure used in the study was the same as the one used in the previous study with the difference that, after introducing errors in the XML file, transferring the file into the Edge™ LINAC, and irradiating the plan, the plan with errors was exported into the ARIA® interface, using ReadDCMPlan software. After exporting the XML files back to the ARIA® interface, the principal organs at risk were selected, and its dose constraints checked. Then, using the External Beam Planning software, the dose volume histograms (DVHs) for each organ at risk selected were analysed. Finally, the volume difference between the reference volume (with zero error) and the volume verified was calculated for each magnitude error, and the graphics regarding this difference, were obtained. In the analysis of the results, three gamma criteria of 1 %/1 mm, 2 %/2 mm, and 3 %/3 mm, were used.

Table 3.7. Information correspondent to the treatment course and dose per fraction for the patient included in the sixth study, Study F.

# Patients	Treatment Course		Dose per Fraction (Gy)
1	Thorax	(1)	2.66

3.2.7 DICOM format

Digital imaging and communication in medicine (DICOM) is the standard format used for management of medical imaging and related data, as well as for communication between different types of medical imaging devices and the computer. DICOM-RT is an extension of the DICOM that is specified for radiotherapy modality and it includes different type of information: (1) DICOM-RT Structure, which describes all the different structures delineated from the planning CT; (2) DICOM-RT Plan, which includes information related to the treatment beams configuration, collimator geometric configuration, and dose prescription; (3) DICOM-RT Dose, which describes the dose distributions calculated; and (4) DICOM-RT Image, which includes the images acquired during the treatment and their related information.

3.2.8 XML file

Extensible markup language (XML) is a markup language that defines a set of rules for encoding documents in a format that is both human-readable and machine-readable, by using tags that can be created and defined by users. XML is specially used to annotate text or additional information, i.e., to outsource data.

3.2.9 ReadDCMPlan

In order to introduce errors in the patient plans, send the patient plans to the LINAC in order to irradiate them, and send them back to the ARIA® interface after irradiation on the LINAC, a software called ReadDCMPlan was developed on the Radiotherapy Department Champalimaud Foundation.

ReadDCMPlan acts on four levels:

1. First, the software reads the patient plan, in DICOM, from the ARIA® interface;
2. Then, the software allows the user to alter the plan parameters by introducing different types of error (MUs, MLC position, and collimator angle);
3. After introducing errors, the software converts the DICOM files with the patient plans, into XML files. These XML files can then be transferred to the LINAC and irradiated on it;
4. Finally, after irradiation, the resultant XML files (with the result of the radiation) can be transferred to the ARIA® interface. For that, the software converts the XML files into DICOM files, format readable by the TPS.

CHAPTER 4. RESULTS AND DISCUSSION

4.1 TrueBeam™ LINAC

4.1.1 QA ArcCHECK vs QA EPID

In the first study, Study A, as mentioned before, the aim was to compare the gamma passing rates values obtained when performing pre-treatment patient-specific QA with ArcCHECK and with EPID, on the TrueBeam™ LINAC, in order to prove that EPID is as good, or even better, than ArcCHECK.

In the first graph, **Figure 4.1**, we see the gamma passing rate values obtained for the composite image, after performing pre-treatment patient-specific QA with ArcCHECK, against the gamma passing rate values obtained after performing pre-treatment patient-specific QA with EPID. Both measurements were made on the TrueBeam™ LINAC. The composite image is the result of the combination of the portal images obtained for each arc of the plan.

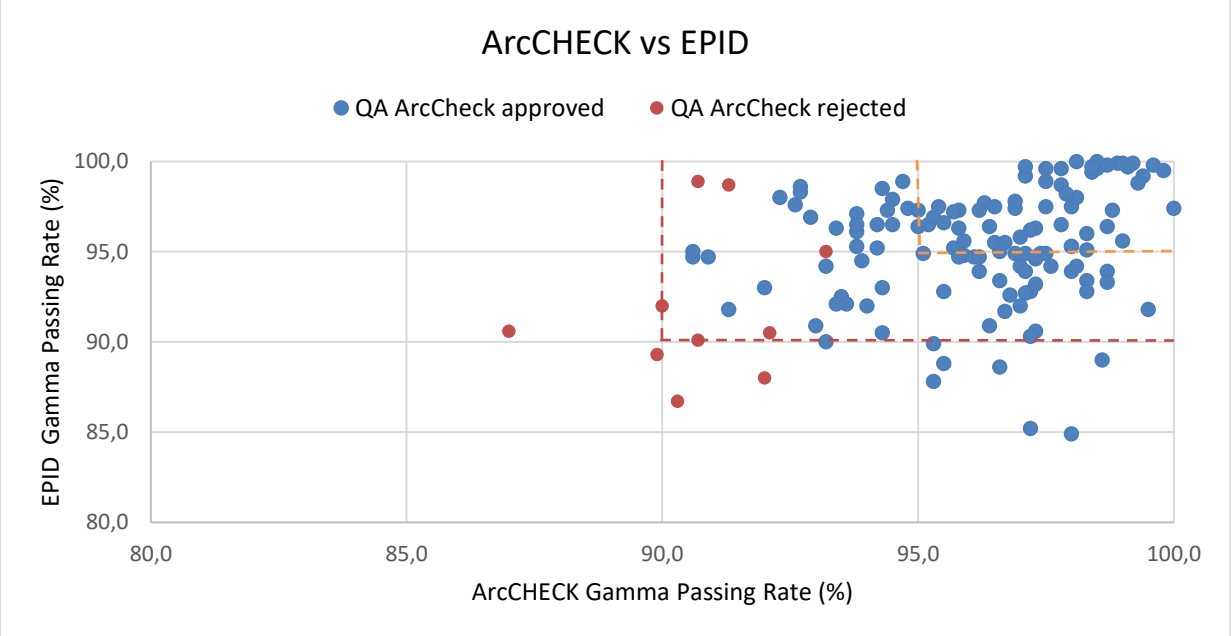

Figure 4.1. Composite gamma passing rate values obtained after performing pre-treatment patient-specific QA with ArcCHECK, against the gamma passing rate values obtained after performing pre-treatment patient-specific QA with EPID. The results were analysed with a 3 %/3 mm gamma criterion. The red line corresponds to the 90 % threshold, while the orange line corresponds to the 95 % threshold.

In the second graphic, **Figure 4.2**, we see the same data as the one shown in **Figure 4.1**, but, this time, separated by type of patient.

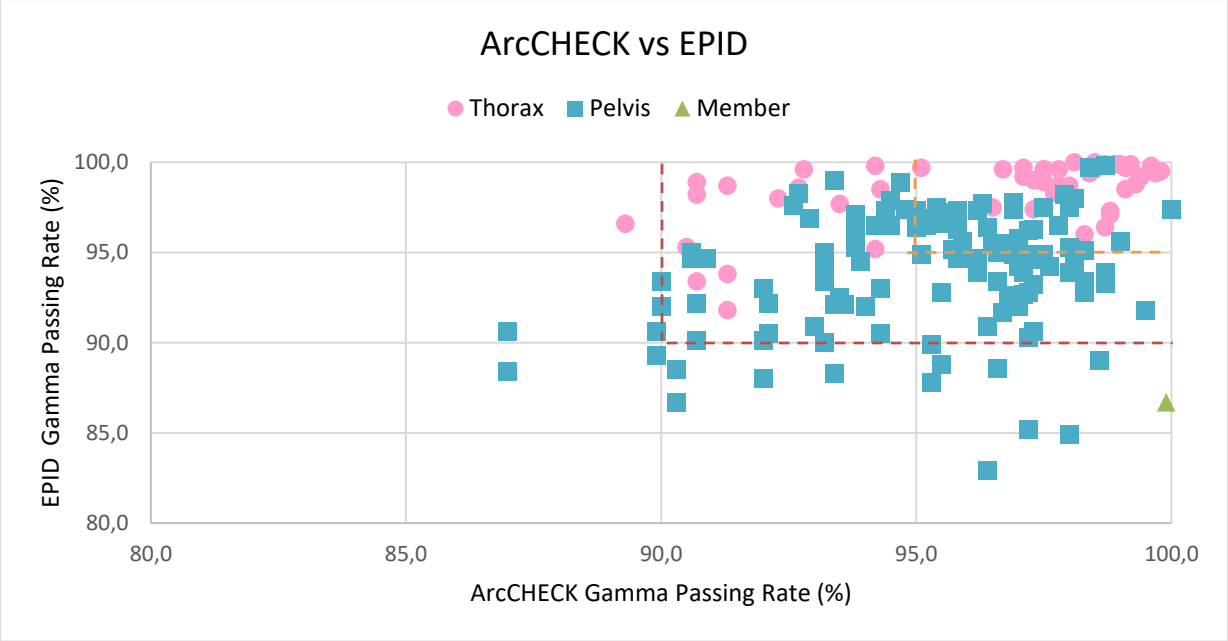

Figure 4.2. Composite gamma passing rate values obtained after performing pre-treatment patient-specific QA with ArcCHECK, against the gamma passing rate values obtained after performing pre-treatment patient-specific QA with EPID, on the TrueBeam™ LINAC, separated by type of patient. The results were analysed with a 3 %/3 mm gamma criterion. The red line corresponds to the 90 % threshold, while the orange line corresponds to the 95 % threshold.

From the analysis of **Figure 4.1**, and for the 140 patient plans approved after performing pre-treatment patient-specific QA with ArcCHECK, we conclude that ArcCHECK allows better results when compared with EPID, once we don't have any gamma passing rate value below 90 % for ArcCHECK, and, for EPID, we have a few. Regarding the 23 patient plans that weren't approved after performing pre-treatment patient-specific QA with ArcCHECK, we conclude that we have higher gamma passing rates when using EPID and, for all cases, the plans that were rejected after performing pre-treatment patient-specific QA with ArcCHECK (due to the gamma passing rate below 90 %) weren't rejected after performing pre-treatment patient-specific QA with EPID.

Regarding **Figure 4.2**, we can see that we have better results for the thorax patients (higher gamma passing rate values), breasts mainly, and worse results for the pelvis patients, prostates mainly. This can be explained by the size of the fields once, for the thorax patients, we usually have bigger fields than for the pelvis patients. Other reason for this can be the different techniques used once for the thorax patients we use IMRT and, for the pelvis patients, we use VMAT. Also, this difference can also be related with the segments, i.e., the plans of the pelvis patients can have higher number of segments than the plans of the thorax patients, explaining the better values obtained for the thorax patients. Finally, another strong hypothesis would be the PDIP algorithm calibrated incorrectly.

It is important to note that most of the results regarding ArcCHECK were already obtained by the time I got at Champalimaud Foundation (due to the pre-treatment patient-specific QA needed and performed with ArcCHECK before each patient treatment), and that the results obtained regarding EPID were only

obtained by me during my project. Thus, the time interval between the different types of measurement can potentially explain some of the differences that we see once there are many factors such as changes on the LINAC output, or changes with the successive interventions and maintenances on the LINAC, that can affect some parameters of the LINAC and, therefore, the measurements performed.

Statistical Data Analysis

Regarding the results obtained, a statistical data analysis was performed using the t-Student test. The t-student test is a statistical test in which the test statistic (t) follows a Student's t-distribution under the null hypothesis [42].

For that, two samples were considered – the one with the measurements performed on ArcCHECK, A, and the one with the measurements performed on EPID, E -, and two different variables were defined – the gamma passing rate obtained for the measurements performed on ArcCHECK, X_A, with a sample mean μ_A, and the gamma passing rate obtained for the measurements performed on EPID, X_E, with a sample mean μ_E. The following hypothesis were formulated:

H0: The results obtained in the two samples are equal, i.e., $\mu_A = \mu_E$

H1: The results obtained for the sample E are better than the ones obtained for the sample A, i.e., $\mu_A < \mu_E$

Thus, in this case, we have a left unilateral t-test, meaning that we will reject the H0 hypothesis if the critic value is higher than the statistic value obtained, i.e., if $t < -t_{critic}$, and we won't reject the H0 hypothesis if the critic value is lower than the statistic value obtained, i.e., if $t > -t_{critic}$.

Using the Excel Data Analysis, and choosing a significance level of 1 %, we could obtain the results shown in **Table 4.1**.

Table 4.1. Results obtained after performing the t-Student test using the Excel Data Analysis.

	X_A	X_E
Média	97.0	97.7
Variância	4.6	8.8
Observações	59	59
Hipótese de diferença de média	0	
gl	105	
Stat t	-1.4	
P(T<=t) uni-caudal	0.1	
t crítico uni-caudal	2.4	
P(T<=t) bi-caudal	0.2	
t crítico bi-caudal	2.6	

Looking for the value obtained for the statistic value t, -1.4, and for the critic value t_{critic}, 2.4, we can conclude that $t > -t_{critic}$ and, therefore, we can't reject the H0 hypothesis with a level of significance of 1 %. In other words, the H0 hypothesis isn't rejected since the value of P for $t = -1.4$ is $P = 0.1 > 0.01$ which is the significance level chosen. This means that the results obtained for the measurements performed on ArcCHECK (sample A) are better than the ones obtained for the measurements performed on EPID (sample E).

4.2 TrueBeam™ LINAC vs Edge™ LINAC

The second study, Study B, aimed compare the average gamma values, as well as the average dose difference values, obtained when performing pre-treatment patient-specific QA with EPID on the two different LINACs (TrueBeam™ LINAC and Edge™ LINAC), with the same plans.

In the first two graphics, **Figure 4.3 (a)** and **(b)**, we see the average gamma values (no units) obtained for each thorax (breast) and pelvis (prostate) patient, respectively, after performing pre-treatment patient-specific QA with EPID on the TrueBeam™ LINAC, against the average gamma values obtained for each prostate (VMAT plans) and breast (IMRT plans) patient, respectively, after performing pre-treatment patient-specific QA with EPID on the Edge™ LINAC. Note that, the values shown correspond to the values obtained after analysing the composite image.

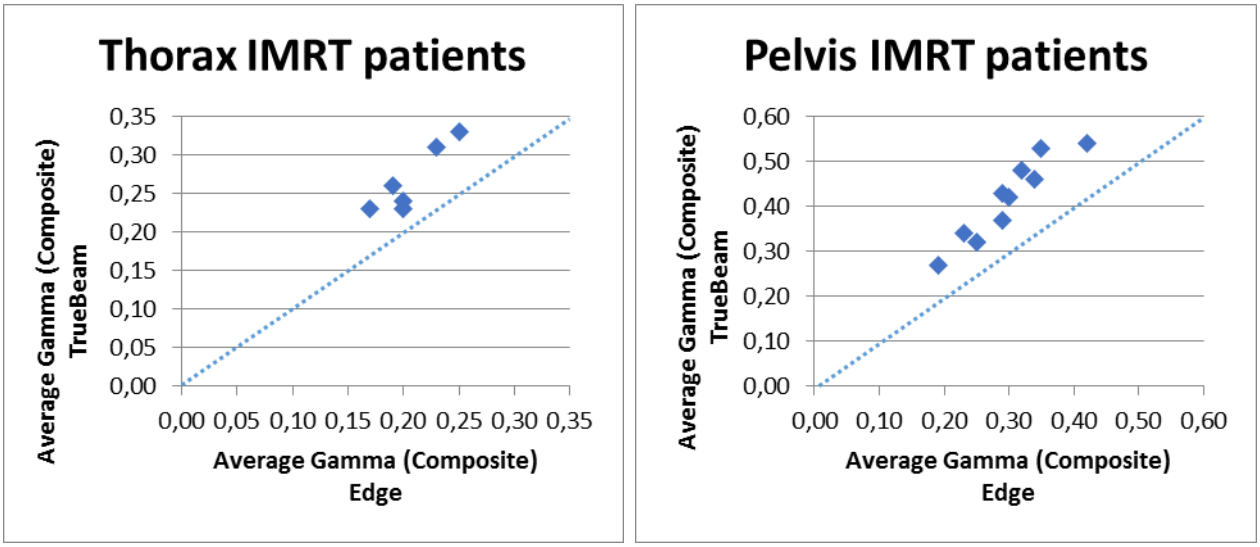

(a) (b)

Figure 4.3. Composite average gamma values (no units) obtained for each (a) thorax and (b) pelvis patient, after performing pre-treatment patient-specific QA with EPID on the TrueBeam™ LINAC, against the average gamma values obtained for the same patient, after performing pre-treatment patient-specific QA with EPID on the Edge™ LINAC. The results were analysed with a 3 %/3 mm gamma criterion.

In the next two graphics, **Figure 4.4 (a)** and **(b)**, we have the values of the average dose difference (CU units, being 1 CU = 1 cGy) obtained for each thorax and pelvis patient, respectively, after performing pre-treatment patient-specific QA with EPID on the TrueBeam™ LINAC, against the values of the average gamma obtained for each thorax and pelvis patient, respectively, after performing pre-treatment patient-specific QA with EPID on the Edge™ LINAC. Note that, again, the values shown correspond to the values obtained after analysing the composite image.

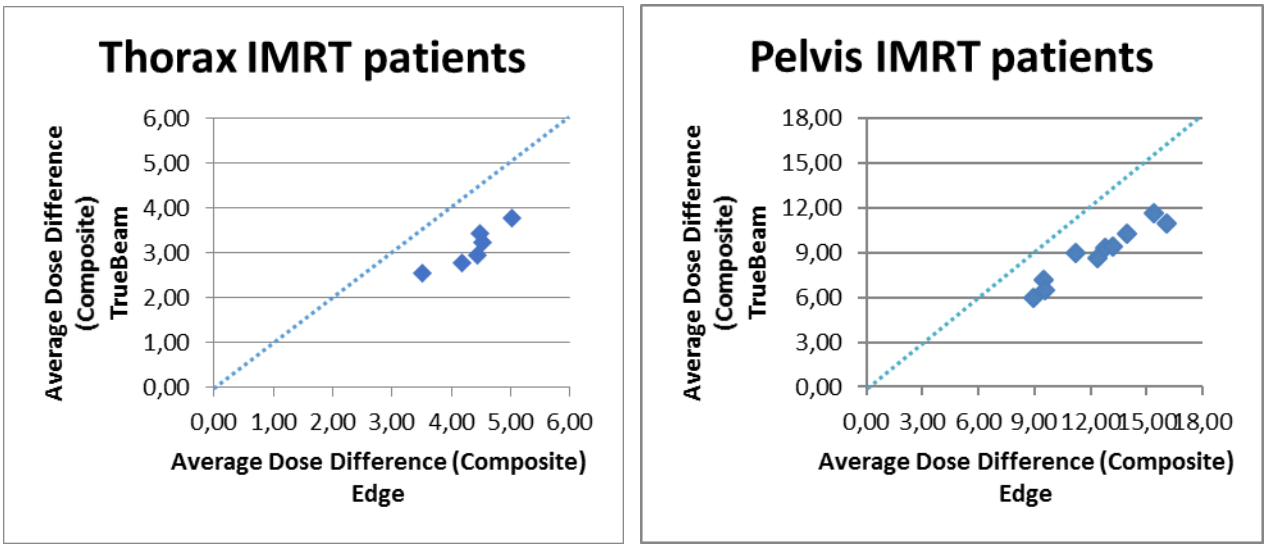

(a) (b)

Figure 4.4. Composite average dose difference values, in CU, obtained for each (a) thorax and (b) pelvis patient, after performing pre-treatment patient-specific QA with EPID on the TrueBeam™ LINAC, against the values of the average gamma obtained for the same patient, after performing pre-treatment patient-specific QA with EPID on the Edge™ LINAC.

Finally, in the next two graphics, **Figure 4.5 (a)** and **(b)**, we have the values of the gamma passing rate obtained for each thorax and pelvis patient, respectively, after performing pre-treatment patient-specific QA with EPID on the TrueBeam™ LINAC, against the values of the average gamma obtained for each thorax and pelvis patient, respectively, after performing pre-treatment patient-specific QA with EPID on the Edge™ LINAC. The values shown correspond to the values obtained after analysing the composite image.

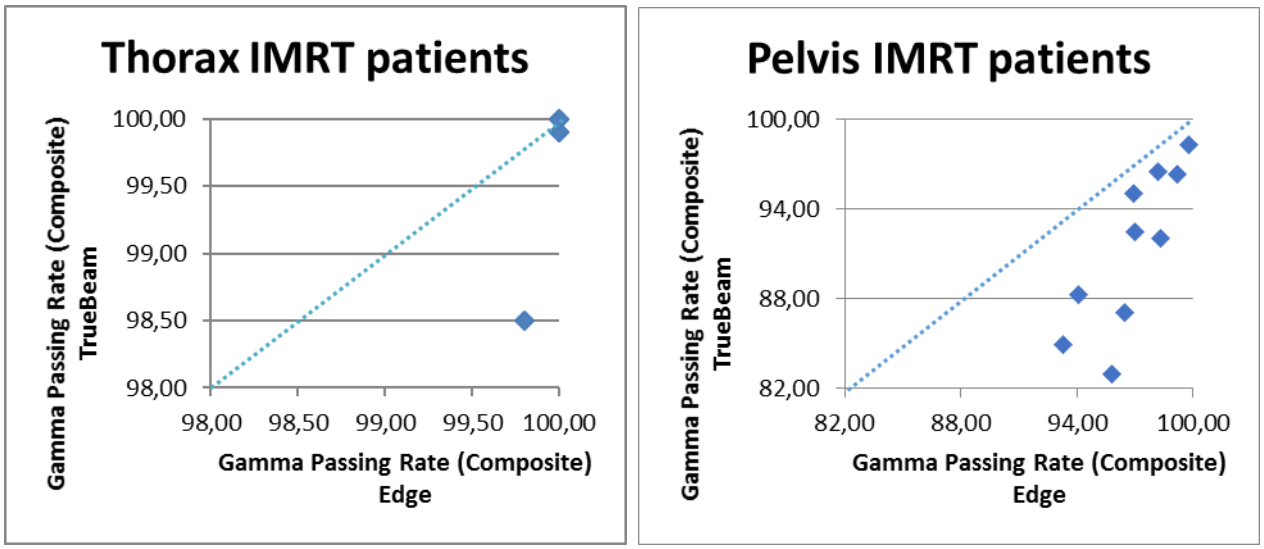

(a) (b)

Figure 4.5. Composite gamma passing rate values obtained for each (a) thorax and (b) pelvis patient, after performing pre-treatment patient-specific QA with EPID on the TrueBeam™ LINAC, against the values of the gamma passing rate obtained for the same patient, after performing pre-treatment patient-specific QA with EPID on the Edge™ LINAC. The results were analysed with a 3 %/3 mm gamma criterion.

From the analysis of **Figure 4.3 (a)** and **(b),** and **Figure 4.4 (a)** and **(b)**, we conclude that, for both thorax and pelvis patients, the results regarding the average gamma are better (lower values) for the Edge™ LINAC, while the results regarding the average dose difference are better (lower values) for the TrueBeam™ LINAC. Thus, the Edge™ LINAC allows better values in terms of average gamma, while the Edge™ LINAC, allows better results in terms of average dose difference. This can be explained by the different a-Si EPIDs incorporated on the two LINACs – the Edge™ LINAC has probably a better EPID than the TrueBeam™ LINAC.

When we analyse the results in terms of gamma passing rate, **Figure 4.5 (a)** and **(b)**, we can conclude that, for both thorax and pelvis patients, we have better results for the Edge™ LINAC. Once again, this can be explained by the better a-Si EPID incorporated in the Edge™ LINAC.

4.3 Edge™ LINAC

4.3.1 QA ArcCHECK vs QA EPID

The aim of the third study, Study C, was, like the first study, to compare the gamma passing rates values obtained when performing pre-treatment patient-specific QA with ArcCHECK and with EPID, on the Edge™ LINAC, in order to prove that EPID is as good, or even better, than ArcCHECK.

In the first graph, **Figure 4.6**, we see the gamma passing rate values obtained for the composite image, after performing pre-treatment patient-specific QA with ArcCHECK, against the gamma passing

rate values obtained after performing pre-treatment patient-specific QA with EPID. Both measurements were made on the Edge™ LINAC.

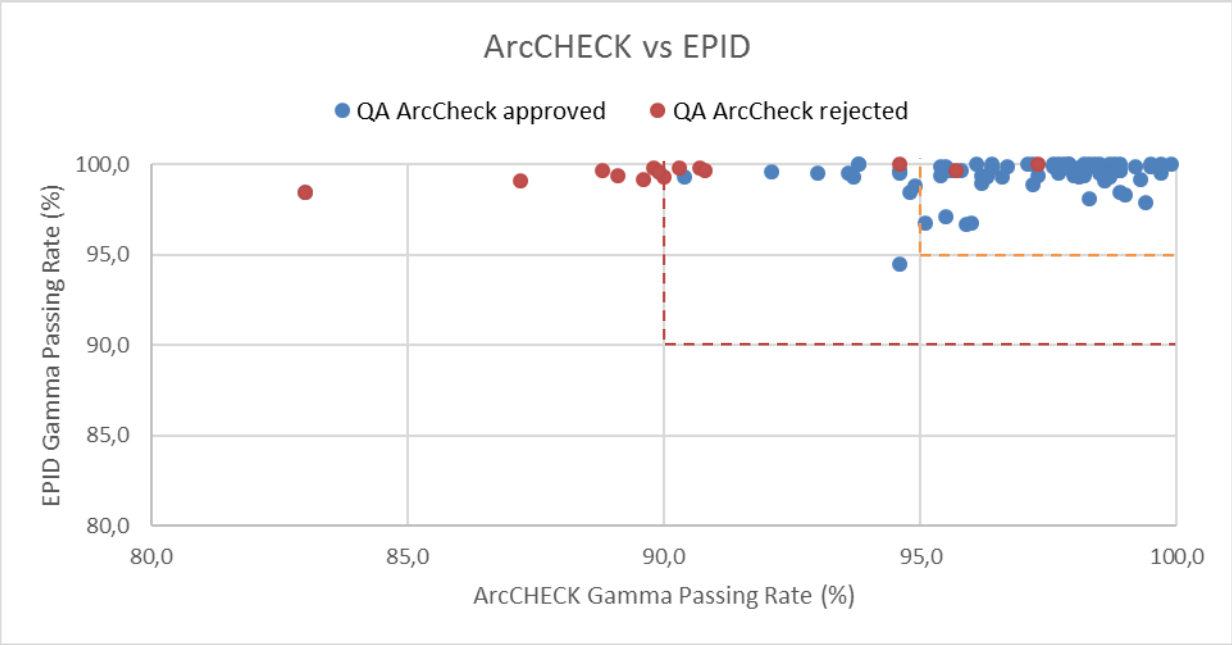

Figure 4.6. Composite gamma passing rate values obtained after performing pre-treatment patient-specific QA with ArcCHECK, against the gamma passing rate values obtained after performing pre-treatment patient-specific QA with EPID, on the Edge™ LINAC. The results were analysed with a 3 %/3 mm gamma criterion. The red line corresponds to the 90 % threshold, while the orange line corresponds to the 95 % threshold.

In the next graphic, **Figure 4.7**, we see the same data as the one shown in the **Figure 4.6**, separated by type of patient.

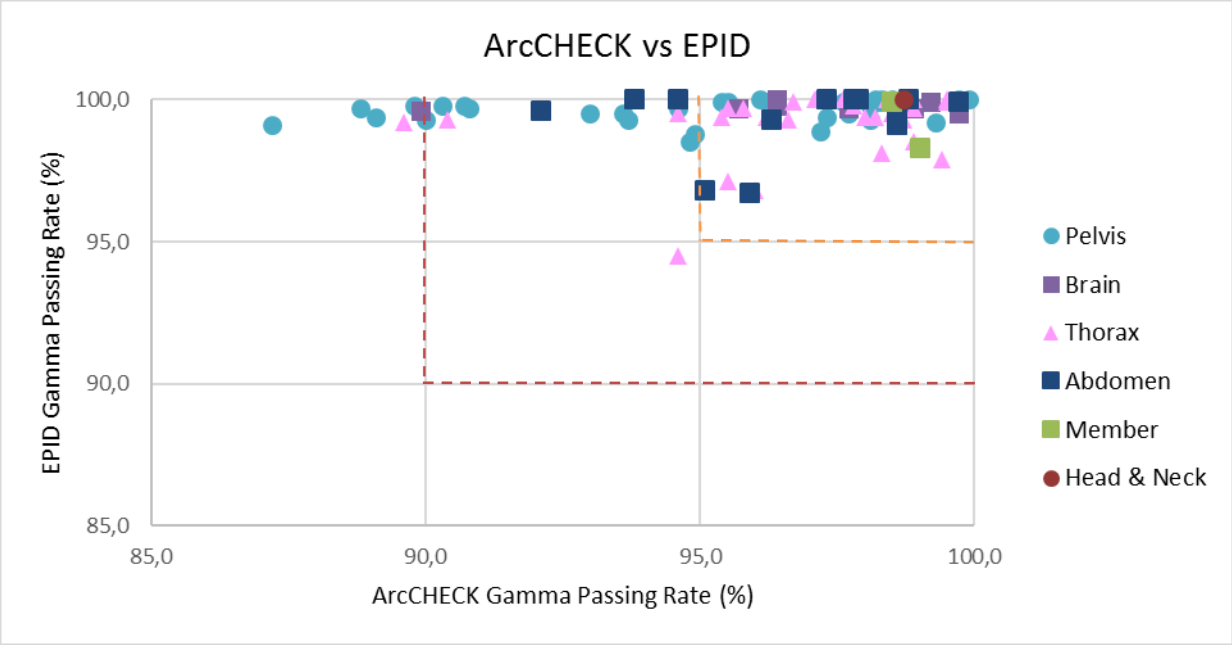

Figure 4.7. Composite gamma passing rate values obtained after performing pre-treatment patient-specific QA with ArcCHECK, against the gamma passing rate values obtained after performing pre-treatment patient-specific QA with EPID, on the Edge™ LINAC, separated by type of patient. The results were analysed with a 3 %/3 mm gamma criterion. The red line corresponds to the 90 % threshold, while the orange line corresponds to the 95 % threshold.

From the analysis of **Figure 4.6**, and for both patient plans approved and rejected after performing pre-treatment patient-specific QA with ArcCHECK, we conclude that EPID allows much better results when compared with ArcCHECK, once we don't have any gamma passing rate value below 90 % for EPID, and for ArcCHECK we have some. This means that all the plans rejected with ArcCHECK were approved with EPID.

Regarding **Figure 4.7**, we can see that, with ArcCHECK, we have better results for thorax patients (higher gamma passing rate values), and worse results for pelvis patients. This can be explained by the size of the fields once, for thorax patients, we usually have bigger fields than for pelvis patients. This would be probably the stronger reason. Other difference can be related with the number of segments, i.e., the plans of pelvis patients can have higher number of segments than the plans of thorax patients, explaining the better values obtained for thorax patients.

Once again it is important to note that most of the results regarding ArcCHECK were already obtained by the time I got at Champalimaud Foundation, and that the results obtained regarding EPID were only obtained by me during my project. Thus, the time interval between the different types of measurement can potentially explain some of the differences that we see once there are many factors such as changes on the LINAC output, or changes with the successive interventions and maintenances on the LINAC, that can affect some parameters of the LINAC and, therefore, the measurements performed.

Statistical Data Analysis

Regarding the results obtained, in the same way as for Study A, a statistical data analysis was performed using the t-Student test (Excel Data Analysis), and choosing a significance level of 1 % (see **Table 4.2**) [42].

Table 4.2. Results obtained after performing the t-Student test using the Excel Data Analysis.

	X_A	X_E
Média	95.9	99.4
Variância	12.7	0.8
Observações	91	91
Hipótese de diferença de média	0	
gl	101	
Stat t	-9.0	
P(T<=t) uni-caudal	0.0	
t crítico uni-caudal	2.4	
P(T<=t) bi-caudal	0.0	
t crítico bi-caudal	2.6	

Looking for the value obtained for the statistic value t, -9.0, and for the critic value t_{critic}, 2.4, we can conclude that $t < -t_{critic}$ and, therefore, we reject the H0 hypothesis with a level of significance of 1 %. In other words, the H0 hypothesis is rejected since the value of P for $t = -9.0$ is $P = 0.0 < 0.01$ which is the significance level chosen. This means that the results obtained for the measurements performed on EPID (sample E) are better than the ones obtained for the measurements performed on ArcCHECK (sample A).

4.3.2 EPID sensitivity

One type patient

In first part of the fourth study, Study D, the aim was to introduce errors in the XML files in order to test the sensitivity of the EPID incorporated on the Edge™ LINAC, i.e., in order to verify if there was any relationship between the values of the average gamma and the magnitude of the error introduced. Four different types of error were introduced - errors in the MUs (%), errors in the MLC position (mm) (random and systematic), and errors in the collimator angle (°).

Initially, the sensitivity of the EPID incorporated on the Edge™ LINAC was tested introducing errors in the MUs. For that, a patient plan was chosen (breast patient) and, in the ReadDCMPlan software, errors in the MUs with 0 %, 2 %, 4 %, 6 %, -2 %, -4 % and -6 % of magnitude were introduced.

In the graphic below, **Figure 4.8**, we have the composite average gamma values obtained in function of the magnitude of error introduced in the MUs, for each counterclockwise (CCW) and clockwise (CW) arcs of the plan.

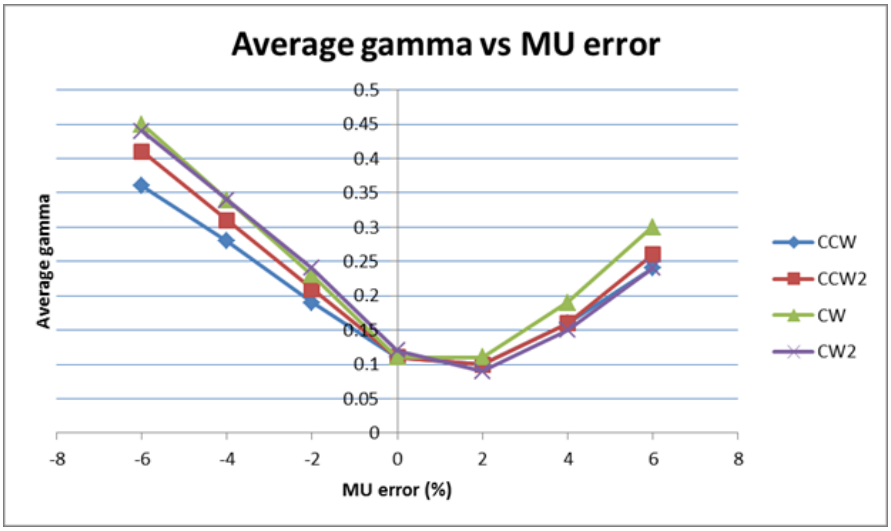

Figure 4.8. Composite average gamma values obtained in function of the magnitude error introduced in the MUs, for each one of the four arcs of the plan (CCW, CCW2, CW, and CW2). The results were analysed with a 3 %/3 mm gamma criterion.

Secondly, the sensitivity of EPID was tested introducing systematic errors in the MLC position. For that, a patient plan was chosen (head and neck patient) and, in the ReadDCMPlan software, errors in the MLC position with 0 mm, 0.5 mm, 1 mm, 2 mm, 3 mm, -0.5 mm, -1 mm, -2 mm, and -3 mm of magnitude were introduced.

In the second graphic, **Figure 4.9**, we have the composite average gamma values obtained in function of the magnitude of error introduced in the MLC position, for each counterclockwise (CCW) and clockwise (CW) arcs of the plan.

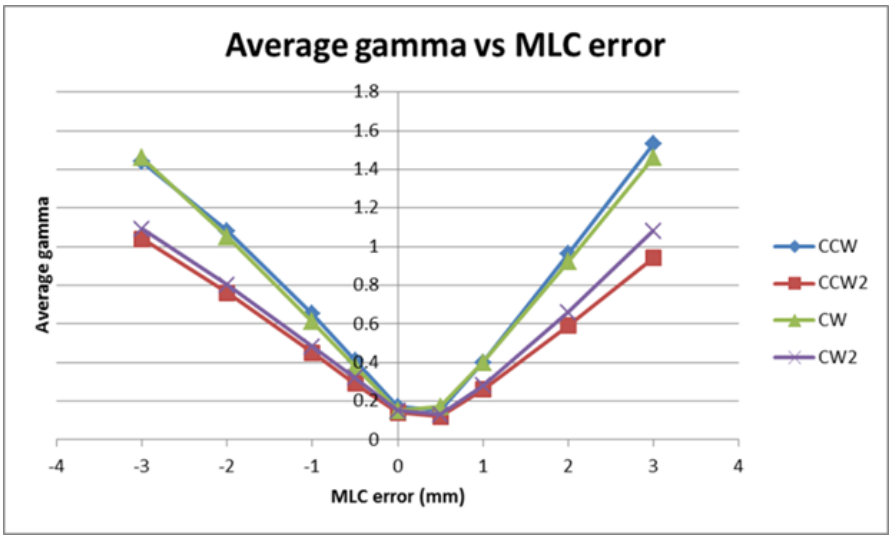

Figure 4.9. Composite average gamma values obtained in function of the magnitude systematic error introduced in the MLC position, for each one of the four arcs of the plan (CCW, CCW2, CW, and CW2). The results were analysed with a 3 %/3 mm gamma criterion.

Thirdly, the sensitivity of EPID was tested introducing, this time, random errors in the MLC position. For that, a patient plan was chosen (pelvis patient) and, in the ReadDCMPlan software, random errors in the MLC position with 0 mm, 1 mm, 2 mm, 3 mm, 4 mm, and 5 mm of magnitude were introduced.

In the next graphic, **Figure 4.10**, we have the composite average gamma values obtained in function of the random magnitude of error introduced in the MLC position, for each counterclockwise (CCW) and clockwise (CW) arcs of the plan.

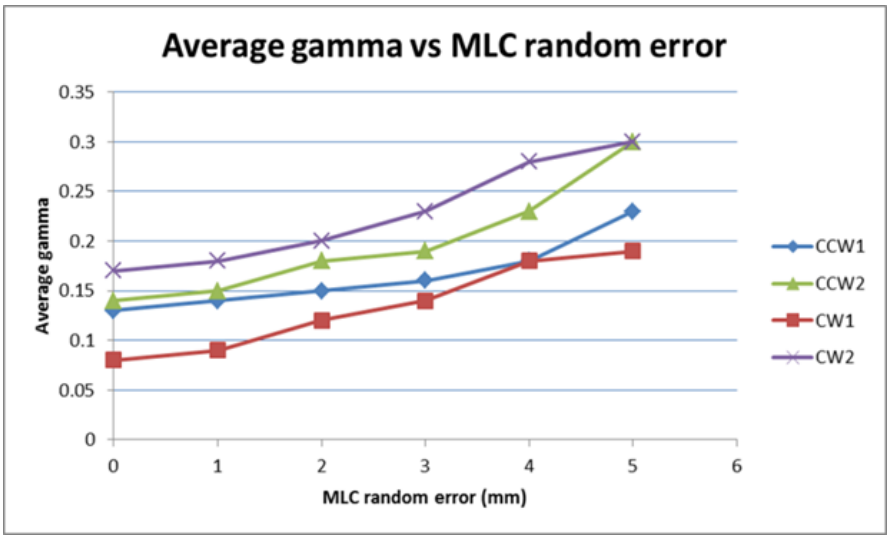

Figure 4.10. Composite average gamma values obtained in function of the magnitude random error introduced in the MLC position, for each one of the four arcs of the plan (CCW1, CCW2, CW1, and CW2). The results were analysed with a 3 %/3 mm gamma criterion.

Finally, the sensitivity of EPID was tested introducing errors in the collimator angle. For that, a patient plan was chosen (brain patient) and, in the ReadDCMPlan software, errors in the collimator angle with 3 °, 2 °, 1 °, 0 °, -1 °, -2 ° and -3 ° of magnitude were introduced.

In the next graphic, **Figure 4.11**, we have the composite average gamma values obtained in function of the magnitude of error introduced in the collimator angle, for each counterclockwise (CCW) and clockwise (CW) arcs of the plan.

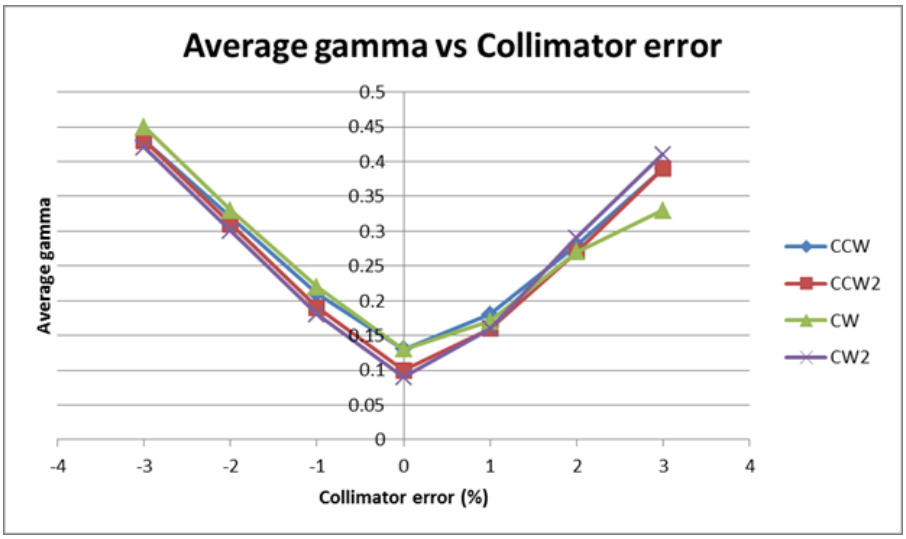

Figure 4.11. Composite average gamma values obtained in function of the error magnitude introduced in the collimator angle, for each one of the four arcs of the plan (CCW, CCW2, CW, and CW2). The results were analysed with a 3 %/3 mm gamma criterion.

From the analysis of **Figure 4.8**, **Figure 4.9**, **Figure 4.10,** and **Figure 4.11**, we conclude that EPID is sensitive to the different types of error introduced once, has we increase the magnitude of the type of error introduced, we get higher and higher values for the average gamma, meaning that the irradiation is worse. Also, in **Figure 4.8**, **Figure 4.9**, and **Figure 4.11**, we note some asymmetry that may be related to the fact that the calibration is not perfect and has some tendency, in this case, to the right, and, therefore, as we increase the magnitude of the errors introduced, that asymmetry becomes even more clear. This asymmetry is suggesting that we are giving systematically underdose.

Different types of patient

The second part of the fourth study, Study D, aimed to introduce errors in the XML files with the patient plans in order to test the sensitivity of the EPID incorporated on the Edge™ LINAC, and compare the results obtained for the different patient plans, and for each type of error introduced. Three different types of error were introduced - errors in the MUs (%), errors in the MLC position (mm) (systematic), and errors in the collimator angle (°).

Initially, the sensitivity of the EPID incorporated on the Edge™ LINAC was tested introducing errors in the MUs, and comparing the results for seven different patients. Errors in the MUs with 0 %, 2 %, 4 %, 6 %, -2 %, -4 % and -6 % of magnitude were introduced.

In the graphic below, **Figure 4.12**, we have the composite average gamma values obtained in function of the magnitude of error introduced in the MUs, for each different type of patient.

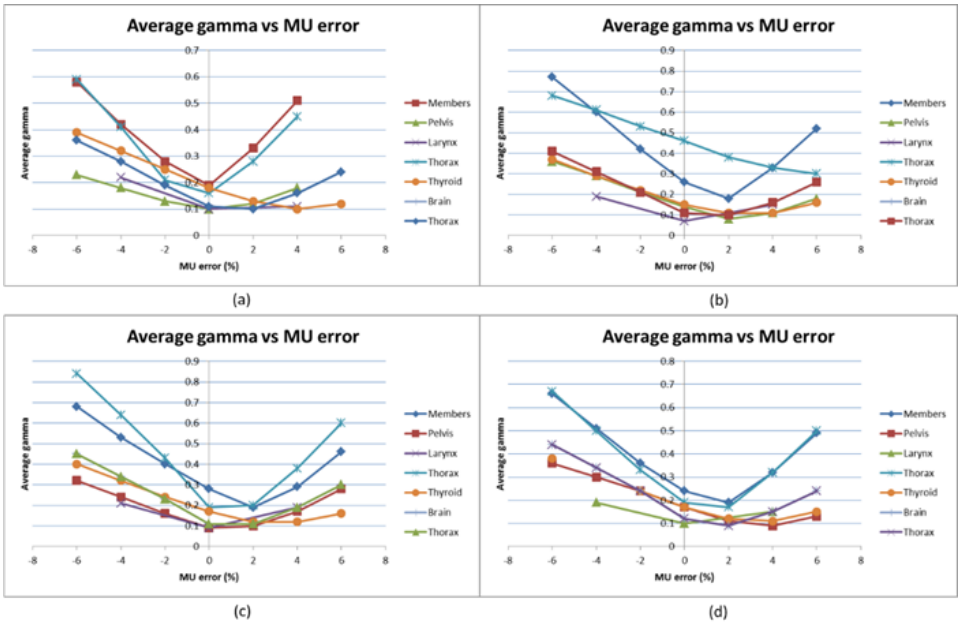

Figure 4.12. Composite average gamma values obtained in function of the magnitude error introduced in the MUs, for different types of patient, and for the (a) CCW arc, (b) CCW2 arc, (c) CW arc, and (d) CW2 arc. The results were analysed with a 3 %/3 mm gamma criterion.

Secondly, the sensitivity of the EPID incorporated on the Edge™ LINAC was tested introducing errors in the MLC position, and comparing the results for nine different patients. Errors in the MLC position with 0 mm, 0.5 mm, 1 mm, 2 mm, 3 mm, -0.5 mm, -1 mm, -2 mm, and -3 mm of magnitude were introduced.

In the next graphic, **Figure 4.13**, we have the composite average gamma values obtained in function of the magnitude of error introduced in the MLC position, for each different type of patient.

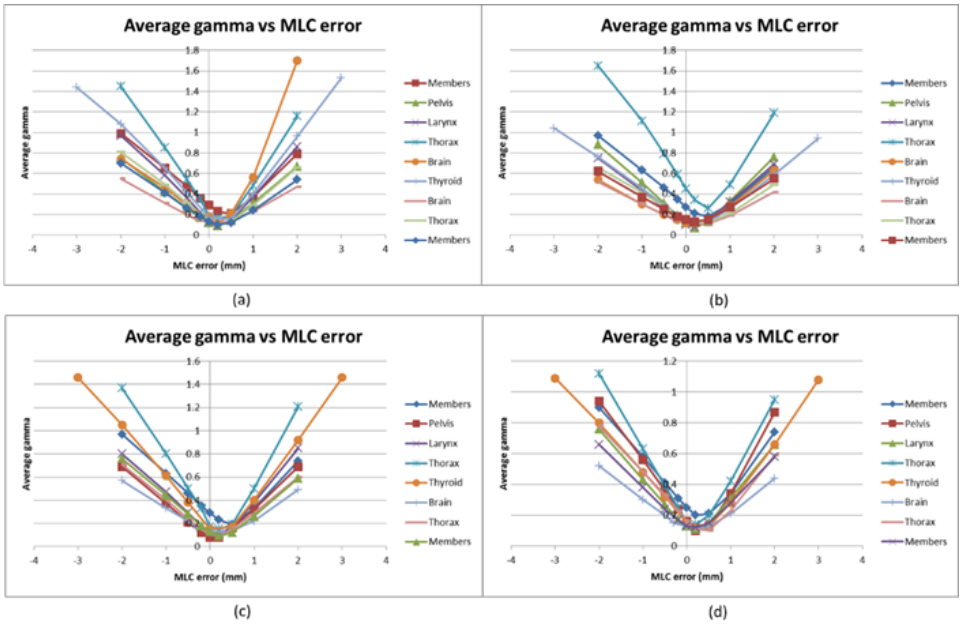

Figure 4.13. Composite average gamma values obtained in function of the magnitude error introduced in the MLC position, for different types of patient, and for the (a) CCW arc, (b) CCW2 arc, (c) CW arc, and (d) CW2 arc. The results were analysed with a 3 %/3 mm gamma criterion.

Finally, the sensitivity of the EPID incorporated on the Edge™ LINAC was tested introducing errors in the collimator angle, and comparing the results for five different patients. Errors in the MLC position with 6 °, 4 °, 2 °, 0 °, -2 °, -4 ° and -6 ° of magnitude were introduced.

In the next graphic, **Figure 4.14**, we have the composite average gamma values obtained in function of the magnitude of error introduced in the collimator angle, for each different type of patient.

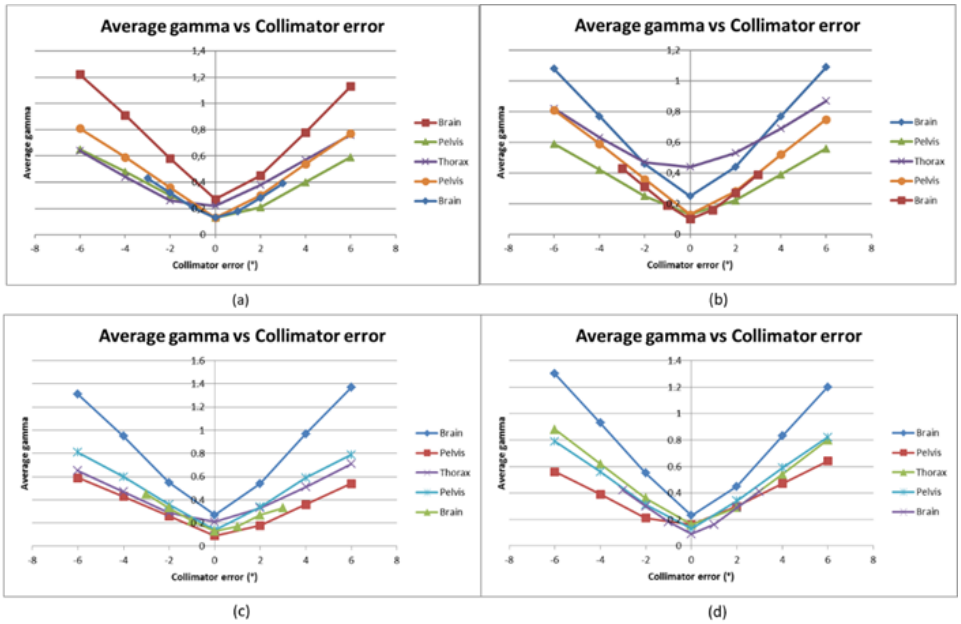

Figure 4.14. Composite average gamma values obtained in function of the magnitude error introduced in the collimator angle, for different types of patient, and for the (a) CCW arc, (b) CCW2 arc, (c) CW arc, and (d) CW2 arc. The results were analysed with a 3 %/3 mm gamma criterion.

From the analysis of **Figure 4.12**, **Figure 4.13**, and **Figure 4.14**, we can conclude once more that EPID is sensitive to the different types of error introduced (as we increase the magnitude of the type of error introduced, we get higher and higher values for the average gamma, meaning that the irradiation is worse). Also, the sensitivity behavior of EPID is pretty similar when considering different types of patient. This is crucial once it shows the stability of EPID.

4.3.3 EPID vs ArcCHECK sensitivity

The sixth study, Study E, aimed to introduce errors in the XML files in order to test the sensitivity of both EPID and ArcCHECK. Four different types of error were introduced - errors in the MUs (%), errors in the MLC position (mm) (random and systematic), and errors in the collimator angle (°) – in four different chosen patients.

Initially, the sensitivity of both systems was tested introducing errors in the MUs. For that, a patient plan was chosen (thorax patient) and, in the ReadDCMPlan software, errors in the MUs with 0 %, 2 %, 4 %, 6 %, -2 %, -4 % and -6 % of magnitude were introduced.

In the graphic below, **Figure 4.15**, we have the gamma passing rate values obtained in function of the magnitude of error introduced in the MUs.

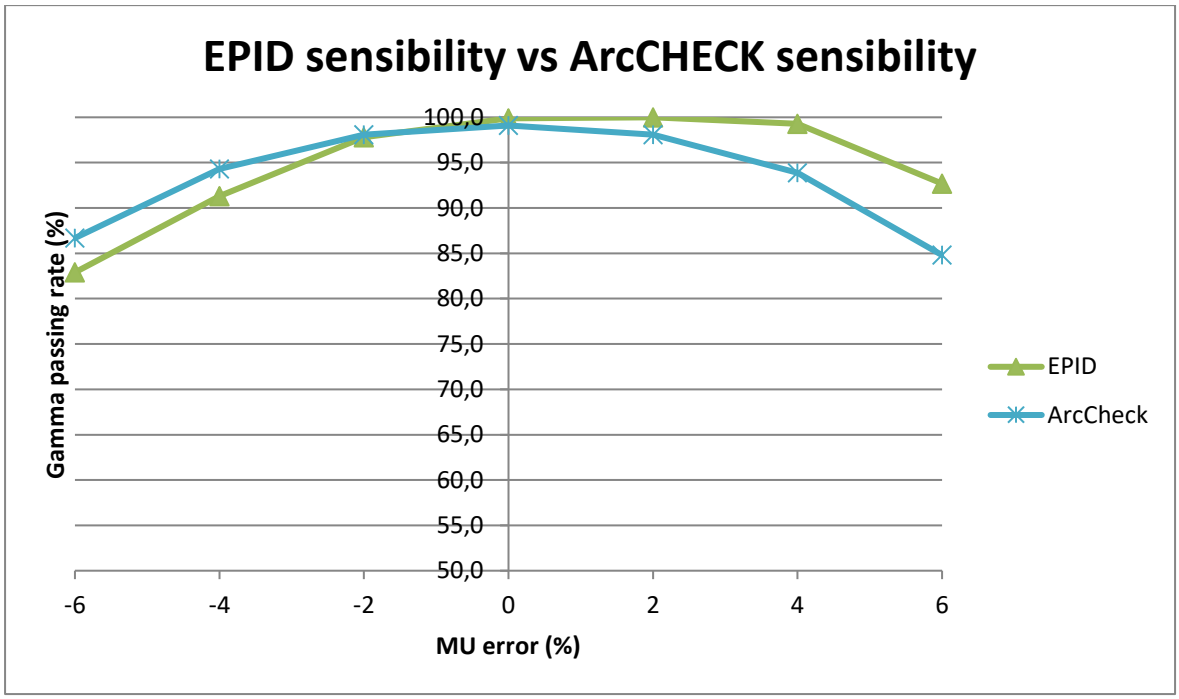

Figure 4.15. Composite gamma passing rate values obtained in function of the magnitude error introduced in the MUs. The results were analysed with a 3 %/3 mm gamma criterion.

Secondly, the sensitivity of EPID was tested introducing errors in the MLC position. For that, a patient plan was chosen (head and neck patient) and, in the ReadDCMPlan software, errors in the MLC position with 0 mm, 0.2 mm, 0.5 mm, 1 mm, 2 mm, -0.2 mm, -0.5 mm, -1 mm, and -2 mm of magnitude were introduced.

In the second graphic, **Figure 4.16**, we have the gamma passing rate values obtained in function of the magnitude of error introduced in the MLC position.

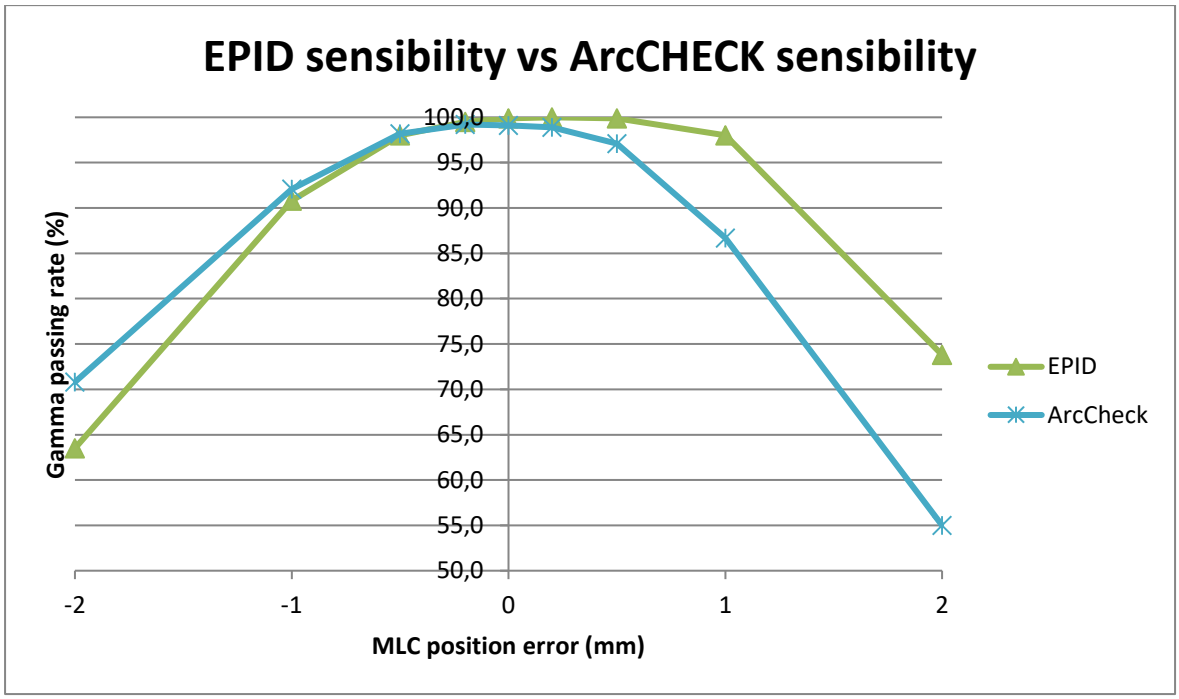

Figure 4.16. Composite gamma passing rate values obtained in function of the magnitude error introduced in the MLC position. The results were analysed with a 3 %/3 mm gamma criterion.

Thirdly, the sensitivity of EPID was tested introducing, this time, random errors in the MLC position. For that, a patient plan was chosen (pelvis patient) and, in the ReadDCMPlan software, random errors in the MLC position with 0 mm, 1 mm, 2 mm, 3 mm, 4 mm, and 5 mm of magnitude were introduced.

In the next graphic, **Figure 4.17**, we have the gamma passing rate values obtained in function of the random magnitude of error introduced in the MLC position.

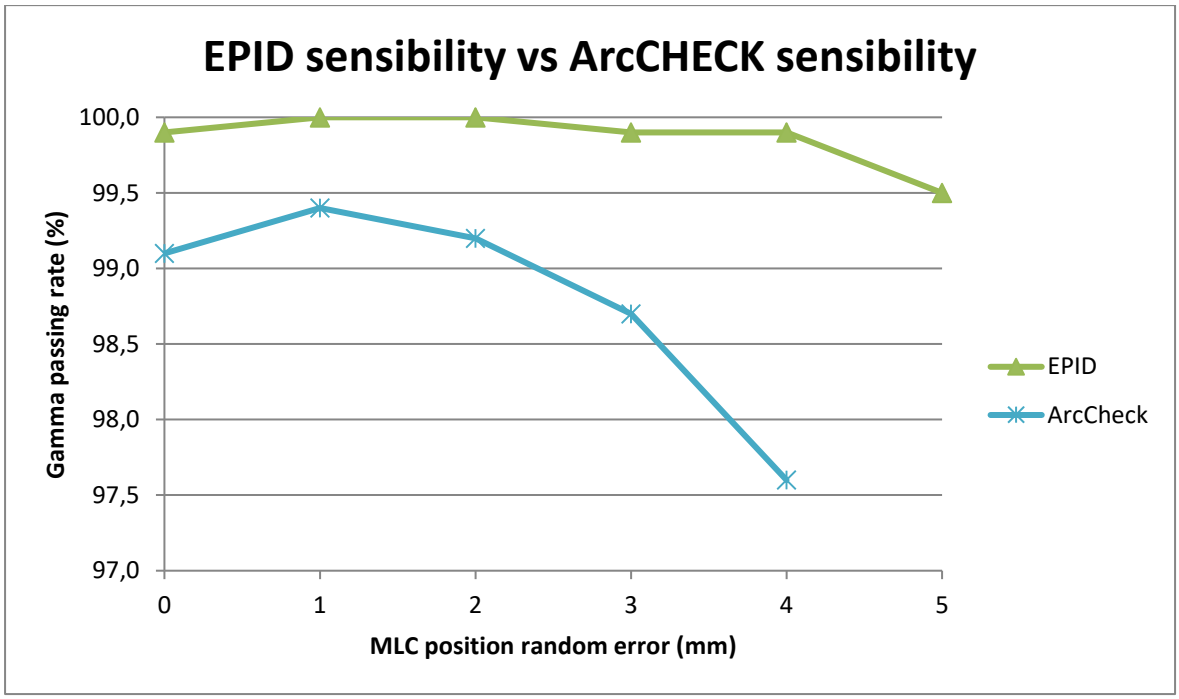

Figure 4.17. Composite gamma passing rate values obtained in function of the random magnitude error introduced in the MLC position. The results were analysed with a 3 %/3 mm gamma criterion.

Finally, the sensitivity of EPID was tested introducing errors in the collimator angle. For that, a patient plan was chosen (brain patient) and, in the ReadDCMPlan software, errors in the collimator angle with 6 °, 4 °, 2 °, 0 °, -2 °, -4 ° and -6 ° of magnitude were introduced.

In the next graphic, **Figure 4.18**, we have the gamma passing rate values obtained in function of the magnitude of error introduced in the collimator angle.

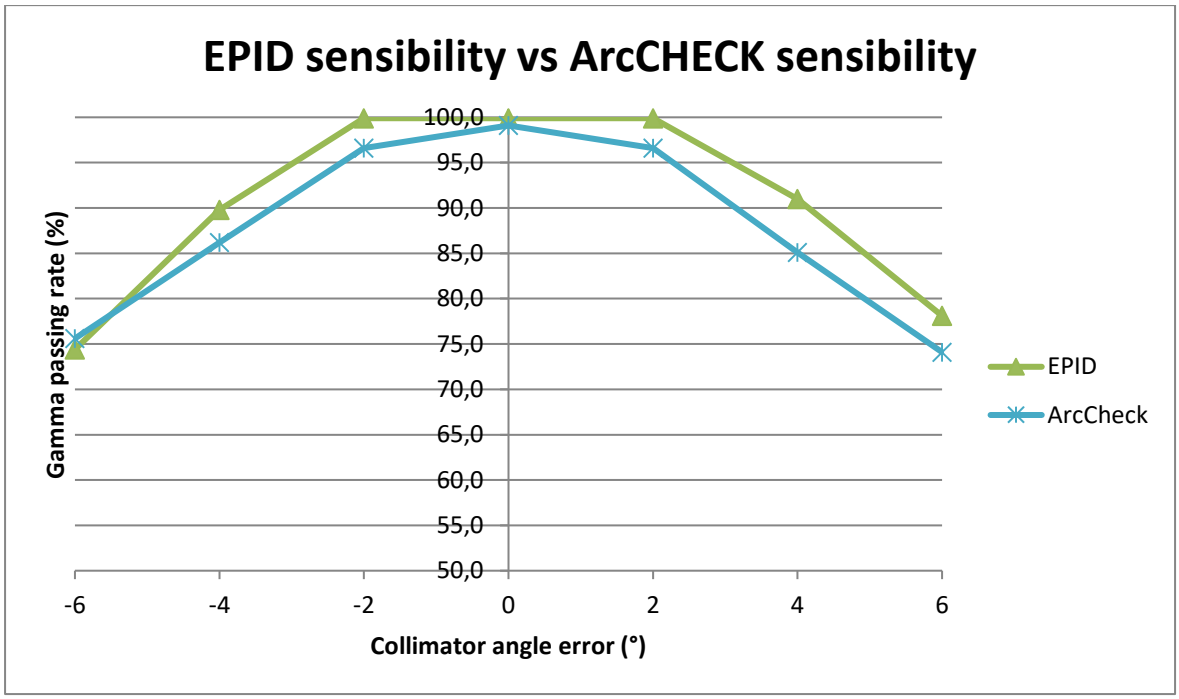

Figure 4.18. Composite gamma passing rate values obtained in function of the error magnitude introduced in the collimator angle. The results were analysed with a 3 %/3 mm gamma criterion.

From the analysis of **Figure 4.15** and **Figure 4.16**, we conclude that, in general, for positive magnitude errors introduced, we have higher gamma passing rate values for EPID, while, for negative magnitude errors introduced, we have higher gamma passing rate values for ArcCHECK. Looking for all the graphics (**Figure 4.15**, **Figure 4.16**, **Figure 4.17**, and **Figure 4.18**) we conclude that, for positive magnitude errors introduced, we have higher gamma passing rate values for EPID. Also, in general, as noted before, we can see some asymmetry that may be related to the fact that the calibration is not perfect and has some tendency, once again, to the right.

In general, it seems that EPID is as sensitive as ArcCHECK and, besides that, shows more coherent results, i.e., the results obtained for EPID are more symmetric (when looking for the same magnitude error with different signals) than the ones obtained for ArcCHECK.

It is important to note that, besides the "strangeness" of the different behavior verified between EPID and ArcCHECK, this was already noted in previous studies. However, the question hadn't been properly answered yet, and the best hypothesis point out towards the LINAC MLC.

4.3.4 Effects in the organs at risk (OARs)

Finally, the aim of the last study was to introduce errors in the XML files and export these plans into the ARIA® interface in order to compare the plans with errors with the ones without errors and,

therefore, verify the effect of the errors in the organs at risk. In this study, 1 patient plan (breast plan) of the 7 patient plans that were irradiated on the Edge™ LINAC, was analysed to make a comparison between the plan with errors and the plan without errors.

In an initial phase, the principal organs at risk were selected, and its dose constraints checked. Then, using the External Beam Planning software, the dose volume histograms (DVHs) for each organ at risk selected were analysed. Finally, the volume difference between the reference volume (with zero error) and the volume verified was calculated for each magnitude error, and the graphics regarding this difference, were obtained.

In the graphic below, **Figure 4.19**, we have the volume difference obtained as function of the gamma passing rate, for each magnitude error introduced. These results concern the principal organ at risk – the left lung – and were obtained after irradiation with EPID.

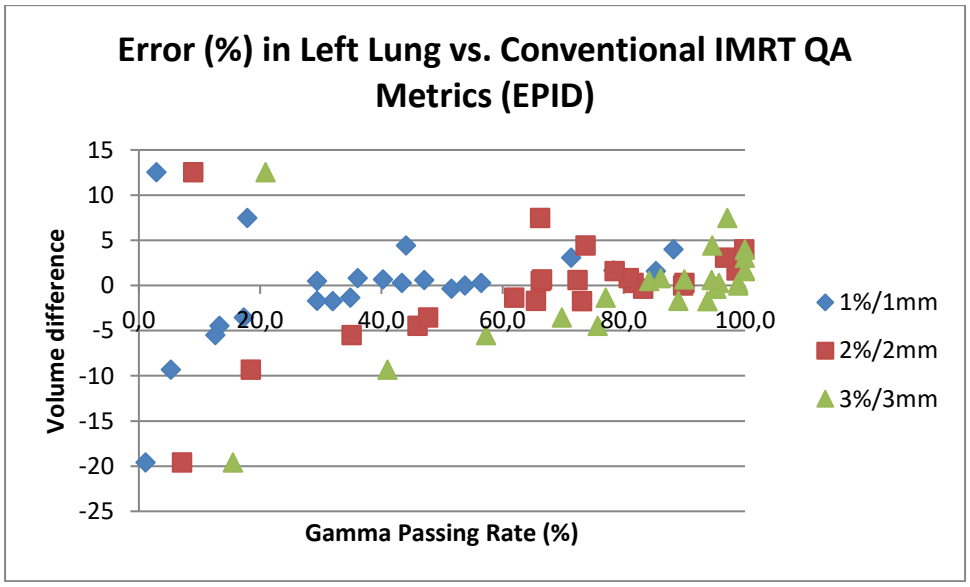

Figure 4.19. Volume difference values in the left lung obtained in function of the gamma passing rate obtained for each error magnitude introduced, and for three different thresholds (1 %/1 mm, 2 %/2 mm e 3 %/3 mm), after irradiation with EPID.

In the second graphic, **Figure 4.20**, we have the volume difference obtained in function of the gamma passing rate, separated by type of error. These results concern the principal organ at risk – the left lung – and were obtained after irradiation with EPID.

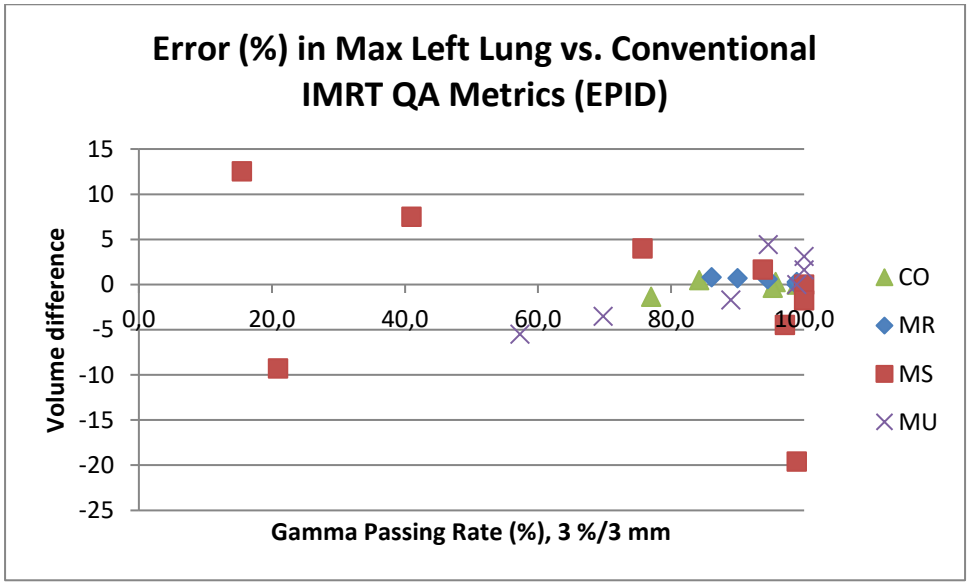

Figure 4.20. Volume difference values in the left lung obtained in function of the gamma passing rate obtained. The values shown are separated by type of error, and were obtained for the 3 %/3 mm threshold, after irradiation with EPID.

In the next graphic, **Figure 4.21**, we have the volume difference obtained in function of the gamma passing rate, for each magnitude of error introduced. These results concern the principal organ at risk – the left lung – and were obtained after irradiation with ArcCHECK.

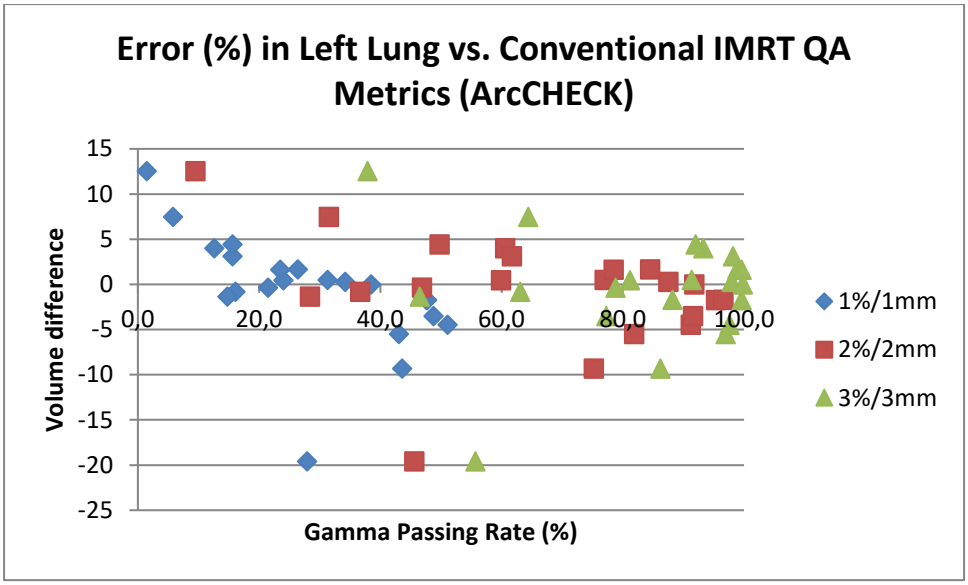

Figure 4.21. Volume difference values in the left lung obtained in function of the gamma passing rate obtained for each error magnitude introduced, and for three different thresholds (1 %/1 mm, 2 %/2 mm e 3 %/3 mm), after irradiation with ArcCHECK.

In the fourth graphic, **Figure 4.22**, we have the volume difference obtained in function of the gamma passing rate, separated by type of error. These results concern the principal organ at risk – the left lung – and were obtained after irradiation with ArcCHECK.

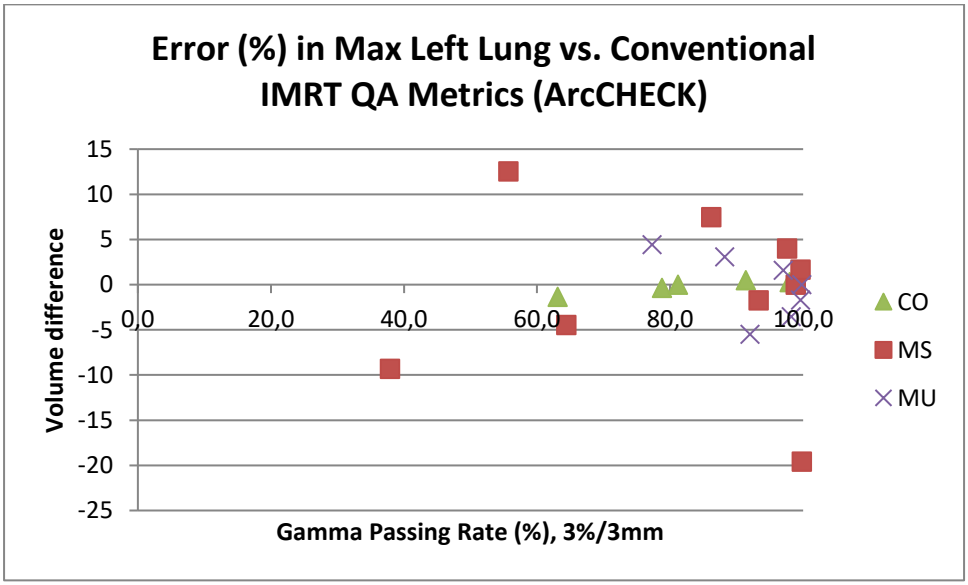

Figure 4.22. Volume difference values in the left lung obtained in function of the gamma passing rate obtained. The values shown are separated by type of error, and were obtained for the 3 %/3 mm threshold, after irradiation with ArcCHECK.

In the next graphic, **Figure 4.23**, we have the volume difference obtained in function of the gamma passing rate, for each magnitude of error introduced. This time, the results concern other principal organ at risk – the heart – and were obtained after irradiation with EPID.

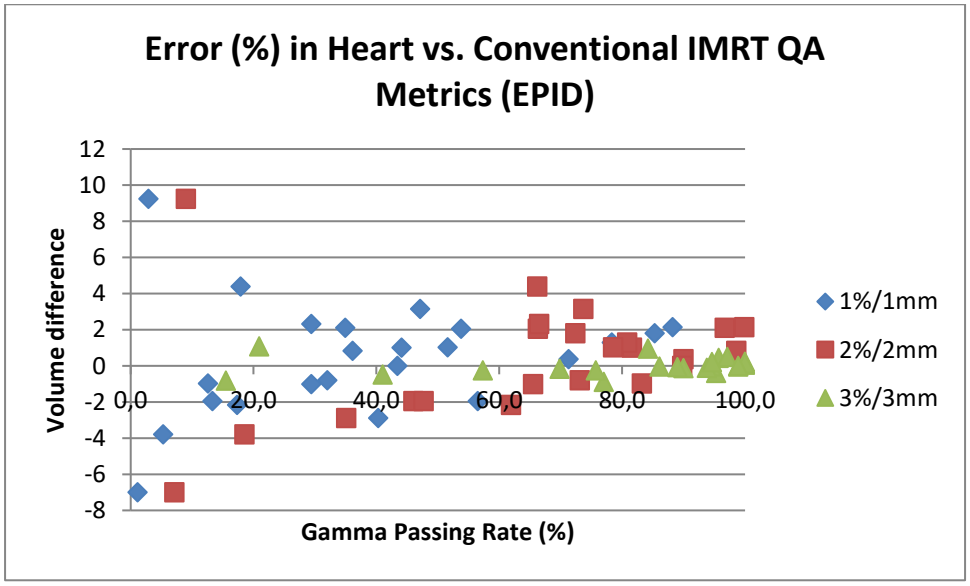

Figure 4.23. Volume difference values in the heart obtained in function of the gamma passing rate obtained for each error magnitude introduced, and for three different thresholds (1 %/1 mm, 2 %/2 mm e 3 %/3 mm), after irradiation with EPID.

In the sixth graphic**, Figure 4.24**, we have the volume difference obtained in function of the gamma passing rate, separated by type of error. These results concern other organ at risk – the heart – and were obtained after irradiation with EPID.

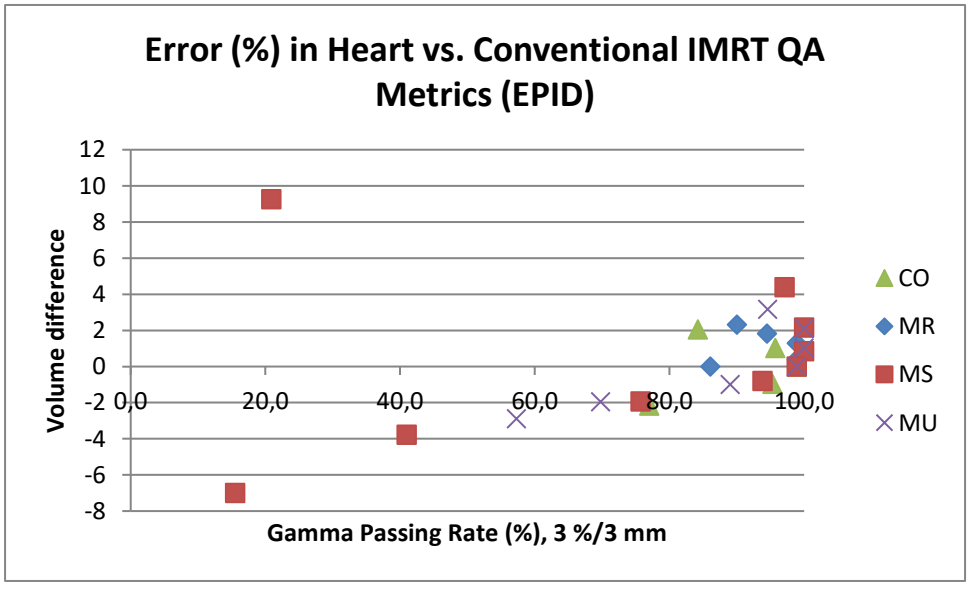

Figure 4.24. Volume difference values in the heart obtained in function of the gamma passing rate obtained. The values shown are separated by type of error, and were obtained for the 3 %/3 mm threshold, after irradiation with EPID.

In the next graphic, **Figure 4.25**, we have the volume difference obtained in function of the gamma passing rate, for each magnitude of error introduced. Once more, the results concern one of the principal organs at risk – the heart – and were obtained after irradiation with ArcCHECK.

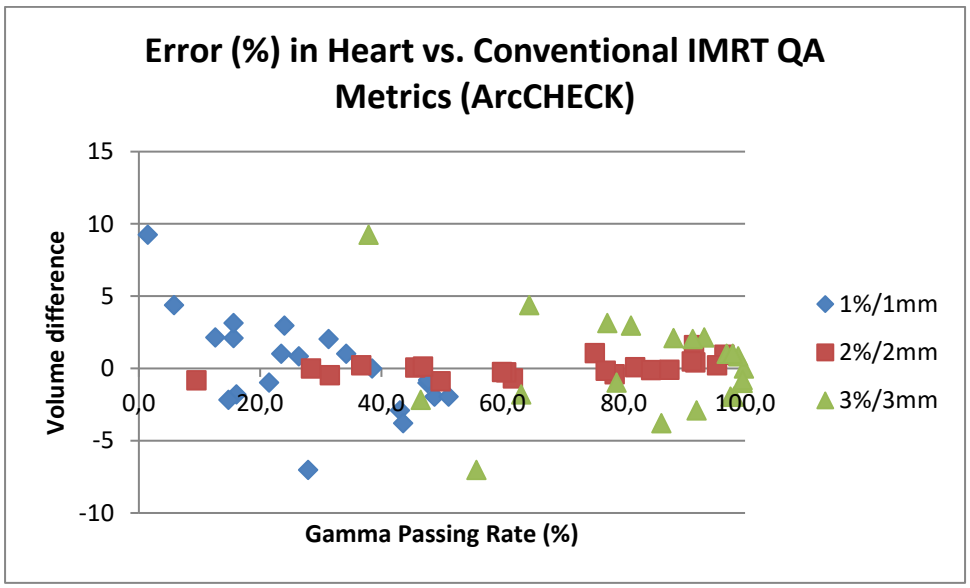

Figure 4.25. Volume difference values in the heart obtained in function of the gamma passing rate obtained for each error magnitude introduced, and for three different thresholds (1%/1 mm, 2%/2 mm e 3%/3 mm), after irradiation with ArcCHECK.

In the final graphic, **Figure 4.26**, we have the volume difference obtained in function of the gamma passing rate, separated by type of error. These results concern other organ at risk – the heart – and were obtained after irradiation with ArcCHECK.

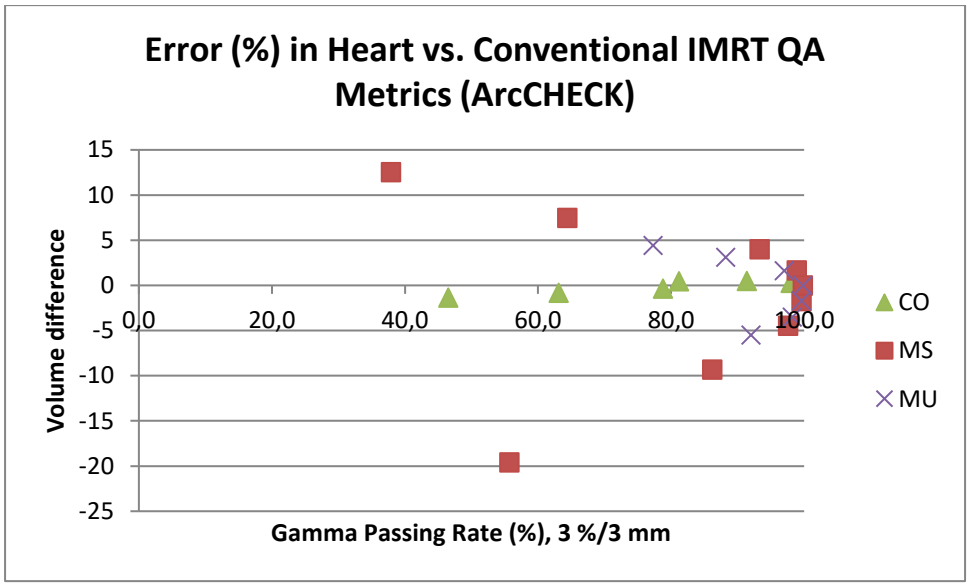

Figure 4.26. Volume difference values in the heart obtained in function of the gamma passing rate obtained. The values shown are separated by type of error, and were obtained for the 3 %/3 mm threshold, after irradiation with ArcCHECK.

Regarding the **Figure 4.19**, **Figure 4.21**, **Figure 4.23**, and **Figure 4.25**, we can conclude that the results agree with the expected once, as we increase the magnitude error introduced, we have higher volume difference values and, therefore, lower gamma passing rate values. In this way, we can conclude that as we increase the magnitude of error introduced, we have higher effects in the organs at risk.

Looking for **Figure 4.20**, **Figure 4.22**, **Figure 4.24**, and **Figure 4.26**, we can conclude that, for both EPID and ArcCHECK, we have similar behaviors for the different types of error introduced. Once more we see the relation that shows the clinical relevance of the gamma passing rate – as we increase the magnitude of the error introduced, we have higher effects in the organs at risk.

CHAPTER 5. CLINICAL INTRODUCTION

By the end of the project (June 2017), given the good results obtained, EPID started to be used routinely in the clinic. For that, some studies were made in order to choose the best parameters to use, namely the gamma passing rate threshold, the SSD distance (distance between EPID and the source) and the values of reference (mean or composite values).

In the next graphic, **Figure 5.1**, we see the gamma passing rate values obtained for the composite image, after performing pre-treatment patient-specific QA with ArcCHECK, against the gamma passing rate values obtained after performing pre-treatment patient-specific QA with EPID, for four different thresholds. All measurements were made on the TrueBeam™ LINAC.

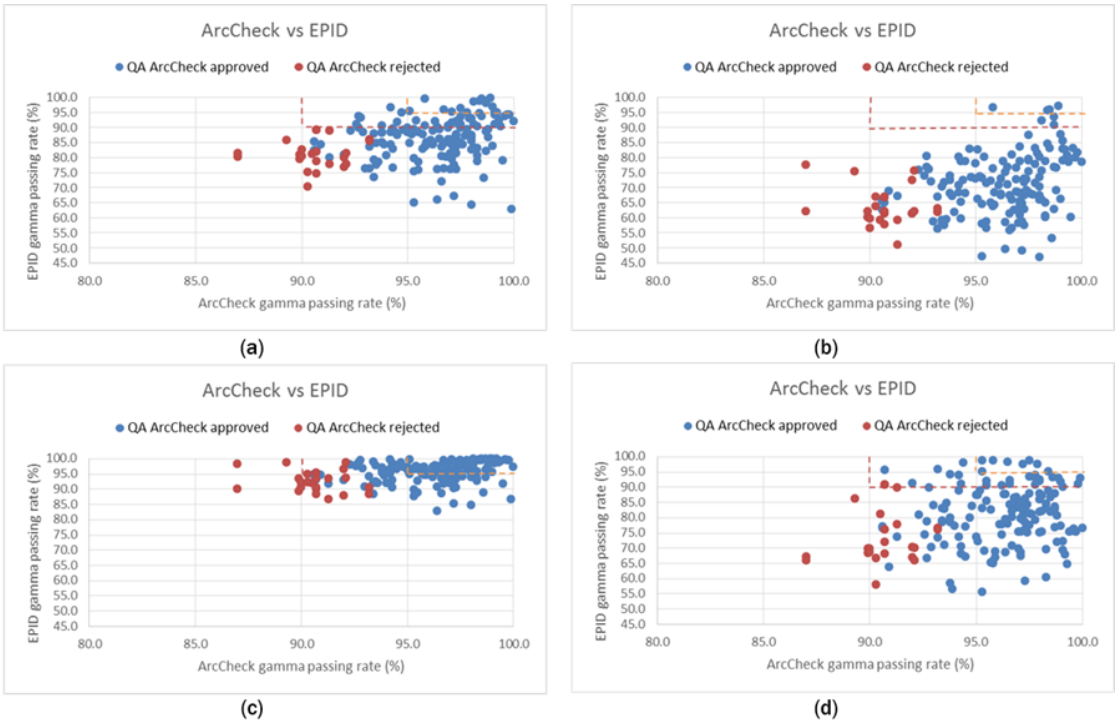

Figure 5.1. Composite gamma passing rate values obtained after performing pre-treatment patient-specific QA with ArcCHECK, against the gamma passing rate values obtained after performing pre-treatment patient-specific QA with EPID, on the TrueBeam™ LINAC, for (a) a 2 %/2 mm threshold, (b) a 2 %/1 mm threshold, (c) a 3 %/3 mm threshold and (d) a 3 %/1 mm threshold. The red line corresponds to the 90 % threshold, while the orange line corresponds to the 95 % threshold.

In the next graphic, **Figure 5.2**, we see the gamma passing rate values obtained for the composite image, after performing pre-treatment patient-specific QA with EPID at a distance of 100 cm from the source, against the gamma passing rate values obtained after performing pre-treatment patient-specific QA with EPID at a distance of 140 cm from the source, on the Edge™ LINAC.

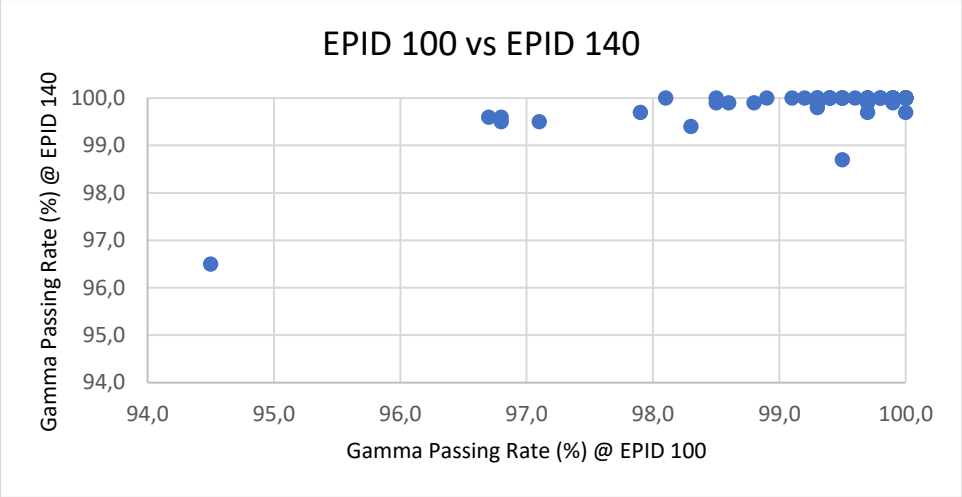

Figure 5.2. Composite gamma passing rate values obtained after performing pre-treatment patient-specific QA with EPID at a distance of 100 cm from the source, against the composite gamma passing rate values obtained after performing pre-treatment patient-specific QA with EPID at a distance of 140 cm, on the Edge™ LINAC.

In the next graphic, **Figure 5.3**, we see the composite gamma passing rate values, against the mean gamma passing rate values, obtained after performing pre-treatment patient-specific QA with EPID, on the Edge™ LINAC.

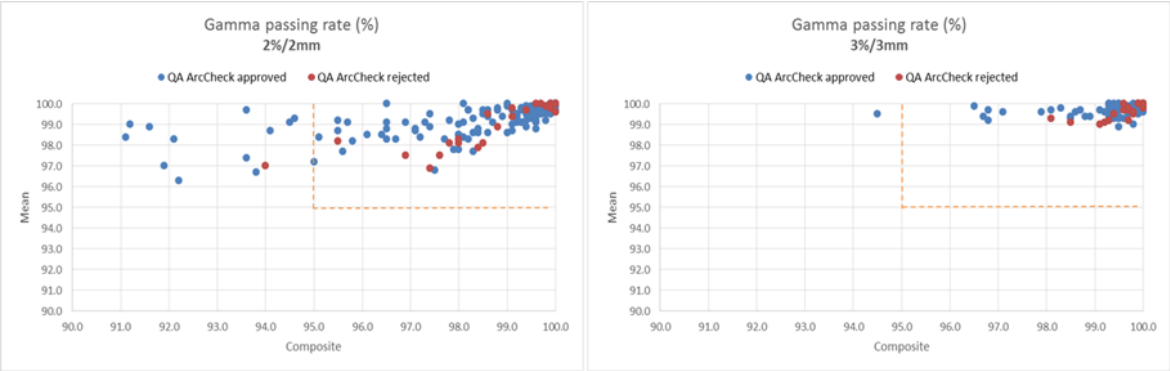

Figure 5.3. Composite and mean gamma passing rate values obtained after performing pre-treatment patient-specific QA with EPID for a (a) 2 %/2 mm threshold and for a (b) 3 %/3 mm threshold. The orange line corresponds to the 95 % threshold.

In the graphic bellow, **Figure 5.4**, we see the (a) composite and the (b) mean gamma passing rate values obtained for the 2 %/2 mm threshold, against the (a) composite and the (b) mean gamma passing rate values obtained for the 3 %/3 mm threshold, obtained after performing pre-treatment patient-specific QA with EPID, on the Edge™ LINAC.

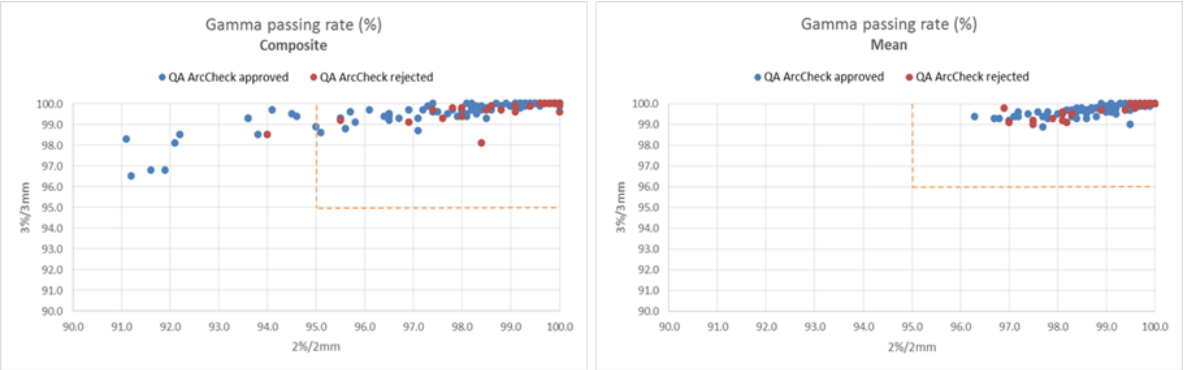

Figure 5.4. (a) Composite and (b) mean gamma passing rate values obtained after performing pre-treatment patient-specific QA with EPID for two different thresholds (2 %/2 mm and 3 %/3 mm). The orange line corresponds to the 95 % threshold.

In the last graphic, **Figure 5.5**, we see the gamma passing rate values obtained for the composite image, after performing pre-treatment patient-specific QA with ArcCHECK, against the gamma passing rate values obtained after performing pre-treatment patient-specific QA with EPID, for (a) a 2 %/2 mm threshold, (b) a 2 %/1 mm threshold, (c) a 3 %/3 mm threshold, and (d) a 3 %/1 mm threshold. All measurements were made on the Edge™ LINAC.

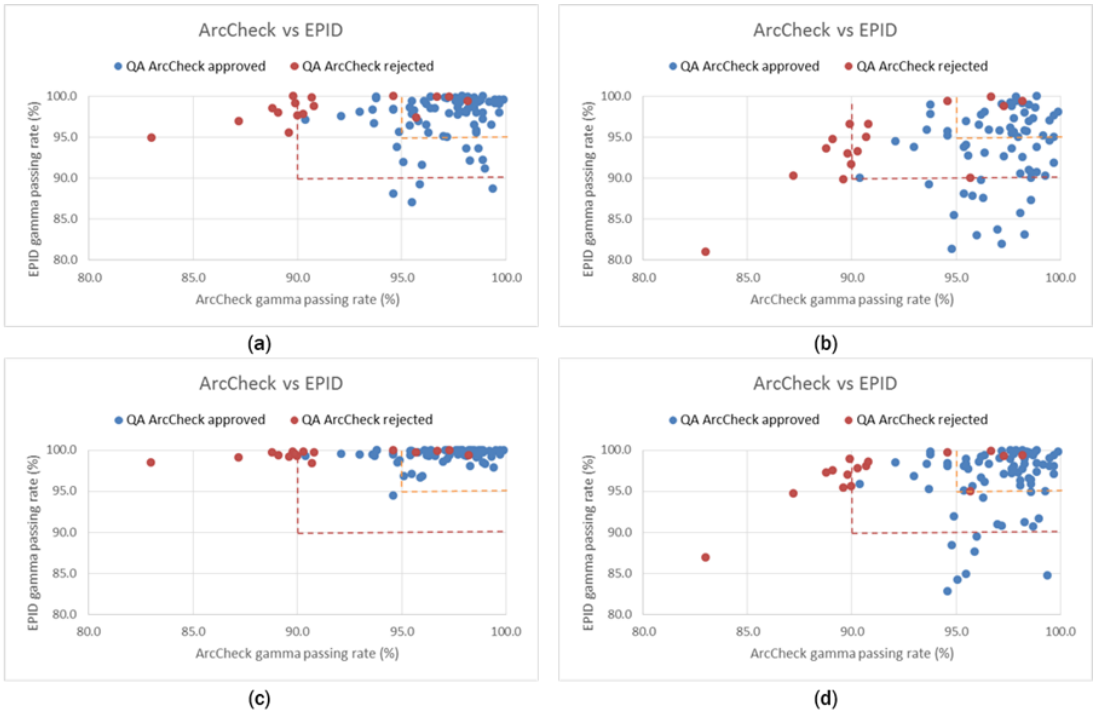

Figure 5.5. Composite gamma passing rate values obtained after performing pre-treatment patient-specific QA with ArcCHECK vs EPID for (a) a 2 %/2 mm threshold, (b) a 2 %/1 mm threshold, (c) a 3 %/3 mm threshold, and (d) a 3 %/ 1 mm threshold. The red line corresponds to the 90 % threshold, while the orange line corresponds to the 95 % threshold.

Looking to **Figure 5.1**, it seems that the 2 %/2 mm threshold 90 % (orange line) is the best threshold once it's the threshold that allows a better ration between the patient plans accepted/rejected. Anyway, once we have decided to start using EPID first only on the Edge™ LINAC (given the not so good results obtained regarding the comparison ArcCHECK/EPID), the question regarding the best threshold to choose was left aside.

According to the results shown in **Figure 5.2** we can see that we have higher gamma passing rate values when we perform pre-treatment patient-specific QA with EPID at a distance of 140 cm from the source. Measuring with EPID at this distance from the source can be a problem once, in the case of having a patient plan with big fields, we can exceed the possible irradiation limits and irradiate EPID. For this reason, the best option is measuring with EPID at a distance of 100 cm from the source (at the EPID level).

From **Figure 5.3**, and **Figure 5.4**, we can conclude that the results are better when we take in account the mean gamma passing rate values, and when considering the 3 %/3 mm threshold. However, the mean gamma passing rate values are not given automatically by the Portal Dosimetry software and that is the reason why we have decided to look for the composite gamma passing rate values (automatically given). Also, the higher results obtained for the 3 %/3 mm threshold are not necessarily better because they are so high that we cannot distinguish between the different cases analysed. For that reason, once again, we concluded that the best choice was the 2 %/2 mm threshold.

Finally, looking for **Figure 5.5** we can conclude that the threshold 2 %/2 mm 90 % is the one that allows better results (rejects all the patient plans rejected with ArcCHECK, and doesn't accept practically all the other cases as for example the 3 %/3 mm threshold).

To sum up, after analysing the results, we have concluded that the best option was to start measuring with EPID first on the Edge™ LINAC and, only after this, on the TrueBeam™ LINAC. The consensual recommendations were to measure with EPID at a distance of 100 cm from the source, use the composite values for a quantitative analysis (and the mean values of each arc values for a more careful analysis), and use the 2 %/2 mm 90 % threshold once this was the more precise one.

CHAPTER 6. CONCLUSION AND FUTURE WORK

With the introduction of advanced irradiation techniques (IMRT and VMAT) in clinical practice, as well as with the prescription of more demanding fractionated schemes, where less irradiation fractions with higher doses per fraction are considered, the accuracy and feasibility of pre-treatment patient-specific QA procedures gains a higher importance. Thus, it is possible to detect, before the patient treatment session starts, human or mechanical errors that could compromise the entire radiotherapy treatment and result in serious injuries.

The potential of EPIDs to perform patient-specific QA has been largely explored due its high resolution and automated acquisition of portal images. In this thesis, initial tests for the implementation of pre-treatment patient-specific QA with EPID were performed, on both Varian LINAC (TrueBeam™ and Edge™) available in the Radiotherapy Department of Champalimaud Foundation.

Regarding the first study, Study A, were the aim was to compare the gamma passing rates values obtained when performing pre-treatment patient-specific QA with ArcCHECK and with EPID, on the TrueBeam™ LINAC, we can conclude that we have better results with ArcCHECK, and for the thorax patients. While the first realization hasn't too much to explain, the second realization can be easily explained by the size of the fields once, for thorax patients, we usually have bigger fields than for pelvis patients, resulting in a worse irradiation of the thorax patients (worse results). Another strong hypothesis would be the Portal Dosimetry algorithm calibrated incorrectly.

In the second study, Study B, which aimed to compare the average gamma values, as well as the average dose difference values, obtained when performing pre-treatment patient-specific QA with EPID, for two different LINACs, we have better results for the average gamma, for both thorax and pelvis patients, on the Edge™ LINAC, and better results for the average dose difference, for both thorax and pelvis patients, on the Edge™ LINAC. This can be explained by the different a-Si EPIDs incorporated on the two LINACs – the Edge™ LINAC has probably a better EPID than the TrueBeam™ LINAC.

Taking in account the third study, Study C, where the aim was, like the first study, to compare the gamma passing rates values obtained when performing pre-treatment patient-specific QA with ArcCHECK and with EPID, on the Edge™ LINAC, we have obtained better results with EPID, and for the thorax patients, lungs mainly. Once again, this can be explained by the size of the fields once, for thorax patients, we usually have bigger fields than for pelvis patients.

In the fourth study, Study D, the aim was to introduce errors in the XML files with the patient plans in order to test the sensitivity of the EPID incorporated on the Edge™ LINAC. For that, different types of error were introduced (MUs, MLC position - random and systematic -, and collimator angle). Given the results obtained, we can conclude that EPID is sensitive to the different types of error introduced (as we increase the magnitude of the type of error introduced, we get higher and higher values for the average gamma, meaning that the irradiation is worse) and that there is some asymmetry that may be related to the

fact that the calibration is not perfect and has some right tendency, in this case, to the right, and, therefore, as we increase the magnitude of the errors introduced (underdose).

The fifth study, Study E, aimed to introduce errors in the XML files in order to test the sensitivity of both EPID and ArcCHECK. After performing the measurements, we concluded that, in general, for positive magnitude errors introduced, we have higher gamma passing rate values for EPID, while, for negative magnitude errors introduced, we have higher gamma passing rate values for ArcCHECK. These results suggest, on the one hand, that EPID is as sensitive as ArcCHECK and, on the other hand, that EPID shows more coherent results (more symmetric results).

Finally, the aim of the sixth and last study, Study F, was to introduce errors in the XML files and export the plans with errors into the ARIA® interface in order to compare the plans with errors with the ones without errors and, therefore, see the effect of the errors in the organs at risk Regarding the results, we can conclude that the obtained is in agreement with the expected once, as we increase the magnitude error introduced, we have higher volume difference values and, therefore, lower gamma passing rate values, meaning that we have higher effects in the organs at risk. Also, for both EPID and ArcCHECK, we have similar behaviors for the different types of error introduced, traducing the clinical relevance of the gamma passing rate.

In the end, the analysis of the results shown that EPID, at the same time, allows better results, and is more sensitivity than ArcCHECK. Besides that, a crucial point differs the two systems – the time dispended performing doing pre-treatment patient-specific QA with EPID is much shorter than the time performing doing pre-treatment patient-specific QA with ArcCHECK. However, more clinical cases, considering several treatment sites and with different fractionation schemes, should be studied with both portal dosimetry and ArcCHECK to verify the obtained results. Said that, the results obtained were very promising and, for the first time at the clinic, due to the results obtained and proved, EPID had started to be used routinely in pre-treatment patient-specific QA in one of the Varian LINAC available (Edge™). Therefore, this only encourages the continuation of the study for implementation of pre-treatment patient-specific QA with EPID on the Varian TrueBeam™ LINAC, as well as the implementation of *in vivo* patient-specific QA.

CHAPTER 7. REFERENCES

[1] S. Nijsten, “Portal Dosimetry in Radiotherapy”. Master Thesis, University of Maastricht, May 2009.

[2] Cancer Treatment Centers of America. What is Brachytherapy?, 2017. (Available at: http://www.brachytherapy.com/)

[3] W. Elmpt, L. McDermott, S. Nijsten, M. Wendling, P. Lambin, B. Mijnheer, “A literature review of electronic portal imaging for radiotherapy dosimetry”, Radiotherapy and Oncology, vol. 88, no. 3, pp. 289-309, Sep 2008.

[4] A. Monti, G. Frigerio, “Dosimetric verification of 6 and 18 MV intensity modulated photon beams using a dedicated fluoroscopic electronic portal imaging device (EPID)”, Radiotherapy and Oncology, vol. 81, no. 1, pp. 88-96, Oct 2006.

[5] M. Herman, “Clinical Use of Electronic Portal Imaging”, Seminars in Radiation Oncology, vol. 15, no. 3, pp. 157-167, Jul 2005.

[6] B. Nelms, K. Rasmussen, W. Tomé, “Evaluation of a fast method of EPID-based dosimetry for intensity modulated radiation therapy”, Journal of Applied Clinical Medical Physics, vol. 11, no. 3, p. 3185, Jan 2011.

[7] E. Podgorsak. Review of Radiation Oncology Physics: A Handbook for Teachers and Students. International Atomic Energy Agency, Vienna, AT, 2005.

[8] C. Dunne-Daly, “Principles of radiotherapy and radiobiology”, Seminars in Oncology Nursing, vol. 15, no. 4, pp. 250–259, Nov 1999.

[9] J. Brown, D. Carlson, D. Brenner, “The tumor radiobiology of SRS and SBRT: Are more than the 5 Rs involved?”, International Journal of Radiation Oncology • Biology • Physics, vol. 88, no. 2, pp. 254–262, Feb 2014.

[10] C. Song, H. Park, R. Griffin, S. Levitt, “Radiobiology of Stereotactic Radiosurgery and Stereotactic Body Radiation Therapy”, Medical Radiology, pp. 51-61, Nov 2011.

[11] N. Suntharalingam, E. Podgorsak, J. Hendry, “Basic Radiobiology”, Radiation Oncology Physics: A Handbook for Teachers and Students, vol. 36. no. 31, p. 485-504, Jul 2005.

[12] RadiologyInfo.org For patients. Linear Accelerator, 2017. (Available at: https://www.radiologyinfo.org/en/info.cfm?pg=linac)

[13] V. Tello, “Medical Linear Accelerators and how they work”. Florida Hospital Cancer InsDtute Kissimmee.

[14] Schoolphysics. The Linear accelerator (LINAC), 2013. (Available at: http://www.schoolphysics.co.uk/age16-19/Medical%20physics/text/Linac_/index.html)

[15] IKnowledge. General and Historical Considerations of Radiotherapy and Radiosurgery, 2015. (Available at: https://clinicalgate.com/general-and-historical-considerations-of-radiotherapy-and-radiosurgery/)

[16] Varian Medical Systems. TrueBeam® Radiotherapy System, 2017. (Available at: https://www.varian.com/oncology/products/treatment-delivery/truebeam-radiotherapy-system)

[17] RadiologyInfo.org For patients. Intensity-Modulated Radiation Therapy (IMRT), 2017. (Available at: https://www.radiologyinfo.org/en/info.cfm?pg=imrt)

[18] Varian Medical Systems. IMRT (Intensity Modulated Radiation Therapy), 2017. (Available at: https://www.varian.com/oncology/treatment-techniques/external-beam-radiation/imrt)

[19] Varian Medical Systems. VMAT: RapidArc®, 2017. (Available at: https://www.varian.com/oncology/treatment-techniques/external-beam-radiation/vmat)

[20] M. Teoh, C. Clark, K. Wood, S. Whitaker, A. Nisbet, “Volumetric modulated arc therapy: a review of current literature and clinical use in practice”, The British Journal of Radiology, vol. 84, no. 1007, pp. 967-996, Nov 2011.

[21] A. Esch, T. Depuydt, D. Huyskens, “The use of an aSi-based EPID for routine absolute dosimetric pre-treatment verification of dynamic IMRT fields”, Radiotherapy and Oncology, vol. 71, no. 2, pp. 223-234, May 2004.

[22] S. Saminathana, V. Chandraraja, C. Sridharb, R. Manickam, “Comparison of individual and composite field analysis using array detector for Intensity Modulated Radiotherapy dose verification”, Thesiss of Practical Oncology & Radiotherapy, vol. 17, no. 3, pp. 157-162, May-Jun 2012.

[23] W. Elmpt, S. Nijsten, B. Mijnheer, A. Dekker, P. Lambin, “The next step in patient-specific QA: 3D dose verification of conformal and intensity-modulated RT based on EPID dosimetry and Monte Carlo dose calculations”, Radiotherapy and Oncology, vol. 86, no. 1, pp. 86-92, Jan 2008.

[24] S. Berry, “Transit Dosimetry for Patient Treatment Verification with an Electronic Portal Imaging Device”. PhD Thesis, Columbia University, 2012.

[25] L. Antonuk, “Electronic portal imaging devices: a review and historical perspective of contemporary technologies and research”, Physics in Medicine & Biology, vol. 47, pp. 31-65, Mar 2002.

[26] R. Charaghvandi, “Redefining radiotherapy for early-stage breast cancer with single dose ablative treatment: a study protocol”, BMC Cancer, pp. 17-181, Mar 2017.

[27] A. Recht, “Postmastectomy Radiotherapy: An American Society of Clinical Oncology, American Society for Radiation Oncology, and Society of Surgical Oncology Focused Guideline Update”, Journal of Clinical Oncology, vol. 34, no. 36, Dec 2016.

[28] D. Low, J. Dempsey, “Evaluation of the gamma dose distribution comparison method”, Medical Physics, vol. 30, no. 9, pp. 2455–2464, Sep 2003.

[29] D. Low, W. Harms, S. Mutic, J. Purdy, “A technique for the quantitative evaluation of dose distributions”, Medical Physics, vol. 25, no. 5, pp. 656–661, Mar 1998.

[30] Elekta. Monaco®, 2017. (Available at: https://www.elekta.com/software-solutions/treatment-management/external-beam-planning/monaco/)

[31] WebMD. Computed Tomography (CT) Scan of the Body, 2017. (Available at: https://www.webmd.com/a-to-z-guides/computed-tomography-ct-scan-of-the-body#1)

[32] C. Talamonti, M. Casati, M. Bucciolini, “Pretreatment verification of IMRT absolute dose distributions using a commercial a-Si EPID”, Medical Physics, vol. 33, no. 11, pp. 4367-4378, Nov 2006.

[33] L. Ma, P. Geis, A. Boyer, “Quality assurance for dynamic multileaf collimator modulated fields using a fast beam imaging system”, Medical Physics, vol. 24, no. 8, pp. 1213–1220, Aug 2008.

[34] A. Curtin-Savard, E. Podgorsak, “Verification of segmented beam delivery using a commercial electronic portal imaging device”, Medical Physics, vol. 26, no. 5, pp. 737–742, May 1999.

[35] K. Pasma, M. Dirkx, M. Kroonwijk, A. Visser, B. Heijmen, “Dosimetric verification of intensity modulated beams produced with dynamic multileaf collimation using an electronic portal imaging device”. Medical Physics, vol. 26, no. 11, pp. 2373–2378, Nov 1999.

[36] J. Chang, G. Mageras, C. Chui, C. Ling, W. Lutz, “Relative profile and dose verification of intensity-modulated radiation therapy”, International Journal of Radiation Oncology • Biology • Physics, vol. 47, no. 1, pp. 231–240, May 2000.

[37] A. Esch, B. Vanstraelen, J. Verstraete, G. Kutcher, H. Dominque, “Pre-treatment dosimetric verification by means of a liquid-filled electronic portal imaging device during dynamic delivery of intensity modulated treatment fields”, Radiotherapy and Oncology, vol. 60, no. 2, pp. 181-190, Aug 2001.

[38] S. Nijsten, B. Mijnheer, A. Dekker, P. Lambin, A. Minken, “Routine individualised patient dosimetry using electronic portal imaging devices”, Radiotherapy and Oncology, vol. 83, no. 1, pp. 65-75, Apr 2007.

[39] K. Pasma, M. Kroonwijk, S. Quint, A. Visser, B. Heijmen, “Transit dosimetry with an electronic portal imaging device (EPID) for 115 prostate cancer patients”, International Journal of Radiation Oncology • Biology • Physics, vol. 45, no. 5, pp. 1297-1303, Dec 1999.

[40] A. Piermattei, A. Fidanzio, G. Stimato, L. Azario, L. Grimaldi, G. D’Onofrio, S. Cilla, M. Balducci, M. Gambacorta, N. Di Napoli, N. Cellini, “In vivo dosimetry by an aSi-based EPID”, Medical Physics, vol. 33, no. 11, pp. 4414–4422, Nov 2006.

[41] A. Piermattei, A. Fidanzio, L. Azario, L. Grimaldi, G. D’Onofrio, S. Cilla, G. Stimato, D. Gaudino, S. Ramella, R. D’Angelillo, “Application of a practical method for the isocenter point in vivo dosimetry by a transit signal”, Physics in Medicine & Biology, vol. 52, no. 16, pp. 5101–5117, Aug 2007.

[42] Wolfram MathWorld. Student's t-Distribution, 2017. (Available at: http://mathworld.wolfram.com/Studentst-Distribution.html)